Available online at www.sciencedirect.com
ScienceDirect
Developmental Biology 317 (2008) 336–353
DEVELOPMENTAL BIOLOGY
www.elsevier.com/developmentalbiology

Histone deacetylase 3 (*hdac3*) is specifically required for liver development in zebrafish

Muhammad Farooq, K.N. Sulochana, Xiufang Pan, Jiawei To, Donglai Sheng, Zhiyuan Gong, Ruowen Ge *

Department of Biological Sciences, National University of Singapore, 117543, Singapore

Received for publication 30 August 2007; revised 14 February 2008; accepted 15 February 2008
Available online 29 February 2008

Abstract

Histone deacetylases (HDACs) are key transcription regulators that function by deacetylating histones/transcription factors and modifying chromatin structure. In this work, we showed that chemical inhibition of HDACs by valproic acid (VPA) led to impaired liver development in zebrafish mainly by inhibiting specification, budding, and differentiation. Formation of exocrine pancreas but not endocrine pancreas was also inhibited. The liver defects induced by VPA correlate with suppressed total HDAC enzymatic activity, but are independent of angiogenesis inhibition. Gene knockdown by morpholino demonstrated that *hdac3* is specifically required for liver formation while *hdac1* is more globally required for multiple development processes in zebrafish including liver/exocrine pancreas formation. Furthermore, overexpression of *hdac3* but not *hdac1* partially rescued VPA induced small liver. One mechanism by which *hdac3* regulates zebrafish liver growth is through inhibiting growth differentiation factor 11 (*gdf11*), a unique target of *hdac3* and a member of the transforming growth factor β family. Simultaneous overexpression or morpholino knockdown showed that *hdac3* and *gdf11* function antagonistically in zebrafish liver development. These results revealed a novel and specific role of *hdac3* in liver development and the distinct functions between *hdac1* and *hdac3* in zebrafish embryonic development.

Keywords: Histone deacetylase; Liver; Pancreas; Organogenesis; Zebrafish; VPA

Introduction

Acetylation and deacetylation of histones generate structural changes in chromatin which play an important role in the control of gene transcription. Histone acetylation promotes the formation of a transcriptional competent environment by 'opening' chromatin. Conversely, histone deacetylation promotes a 'closed' chromatin state and transcriptional repression (Cheung et al., 2000).

Histone deacetylases (HDACs) deacetylate histones and certain transcription factors. Eighteen mammalian HDACs have been identified to date and they are classified into three classes based on sequence homology to different yeast HDACs. Class I HDACs (HDAC1, 2, 3 and 8) are most closely related to the yeast HDAC RPD3. Class II HDACs (HDAC4, 5, 6, 7, 9 and 10) are highly homologous to yeast HDA1. Class III HDACs are most similar to yeast Sir2 HDAC. While class I HDACs are expressed in most cell types, the expression pattern of class II HDACs is more restricted, and has been shown to be involved in cell differentiation and developmental processes such as myogenesis (de Ruijter et al., 2003).

Because of the relatively ubiquitous expression pattern of class I HDACs and the fundamental roles HDACs play in regulating chromatin structure, it was perceived that class I HDACs would play a general role in embryonic development. However, recent findings indicate otherwise. Global gene expression profiling in *C. elegans* identified tissue-specific and extracellular matrix (ECM)-related genes as major HDAC1 targets (Whetstine et al., 2005). In mouse, HDAC1 and 2 are expressed in the prospective epithelium of the developing intestine, regulating intestine epithelial differentiation (Tou et al., 2004). Recently, HDAC3 expression was reported to be

* Corresponding author.
E-mail address: dbsgerw@nus.edu.sg (R. Ge).

0012-1606/$ - see front matter © 2008 Elsevier Inc. All rights reserved.
doi:10.1016/j.ydbio.2008.02.034

restricted to the proliferative compartment of mouse small intestine and colon (Wilson et al., 2006). In zebrafish, *hdac1* has been shown to play specific roles in neurogenesis, craniofacial cartilage and pectoral fin development (Cunliffe, 2004; Phiel et al., 2001; Yamaguchi et al., 2005). However, the functions of other class I HDACs in zebrafish embryonic development are not known.

Recently, significant advances have been made in our understanding of the molecular mechanisms that control vertebrate liver development. During early development of the zebrafish digestive system, a number of buds emerge from the gut primordium, giving rise to different organs including liver and pancreas (Field et al., 2003). Initial patterning events define the liver precursors within the foregut endoderm. This hepatic primordium later forms a morphologically distinct bud at around 28–30 hpf that grows out from the foregut. The growth phase follows the completion of budding and is characterized by change in liver size and shape. However, a lot still remains unknown of liver organogenesis. In mouse, early liver budding requires mesodermal inductive signals such as fibroblast growth factors (FGFs) from the adjacent cardiogenic mesoderm and bone morphogenic proteins (BMPs) from nearby septum transversum mesenchyme. In addition, interaction with endothelial cells is also crucial although the signaling molecules from endothelial cells are not known at the moment (Zaret, 2002). In contrast, endothelial cells are not necessary for liver budding in zebrafish because in the mutant *cloche* which lacks most endothelial cells, liver buds normally (Field et al., 2003).

HDAC inhibitors have been reported to induce Hepatoma cell growth arrest, apoptosis and hepatocyte differentiation in vitro, but their role in hepatocyte differentiation in vivo has not been investigated (Herold et al., 2002; Yamashita et al., 2003).

In this work, we analyzed the roles of HDACs, in particular *hdac1* and *hdac3*, in zebrafish embryonic development especially liver development. We found that inhibiting HDACs with HDAC inhibitors valproic acid (VPA) and Trichostatin A (TSA) not only led to defects in angiogenesis, but also interfered with liver and exocrine pancreas formation, while the endocrine pancreas was not affected. Hepatoblast markers (*prox1*, *hhex*, *foxa3*) were absent or severely reduced in the liver region in treated embryos, while marker genes for hepatocyte differentiation *ceruloplasmin* (*Cp*) and *liver faty acid binding protein* (*lfabp*) were not expressed in liver until 4–5 dpf. We demonstrated that the liver defects are not related to the vascular defect. Gene knockdown with morpholino antisense oligonucleotide (MO) indicated that although both *hdac3* and *hdac1* are required for liver formation in zebrafish, *hdac3* plays a more specific role. We further demonstrated that one mechanism of *hdac3* function is by suppressing growth differentiation factor 11 (*gdf11*) gene, a negative regulator of cell proliferation and a specific transcriptional target of *hdac3* (Zhang et al., 2004). Our results provide the first evidence that HDACs are required for liver/exocrine pancreas formation and revealed a novel role of *hdac3* in liver organogenesis.

Materials and methods

Zebrafish and embryos

Local outbreed wild type (WT) as well as transgenic lines of zebrafish and embryos was maintained, collected and staged as described (Westerfield, 1995). Transgenic lines used are *Tg(lfabp:RFP; elaA:EGFP)* containing liver-specific *liver fatty acid binding protein* (*lfabp*) promoter controlled RFP and exocrine pancreas-specific *elastase A* (*elaA)* promoter controlled EGFP (Her et al., 2003; Wan et al., 2006); *Tg(fli-1:EGFP)* in which GFP is expressed in endothelial cells (Lawson and Weinstein, 2002).

Treatment of embryos with inhibitors of HDACs and angiogenesis

VPA (Sodium 2-propylpentanoate) and TSA were purchased from Sigma Aldrich, and Valpromide (VPM, Dipropylacetamide) was a kind gift from Katwijk Chemie BV, Netherlands. Angiogenesis inhibitors SU5614, SU1498, 2-methoxyestradiol and Genestein were purchased from Calbiochem. Embryos were raised up to the shield stage and HDAC or angiogenesis inhibitors were then added to embryo water (RO water supplemented with 40 mg/ml ocean salt) after dissolving either in water (VPA) or DMSO (TSA, SU5614, SU1498, 2-methoxyestradiol and Genestein). The embryo water was replaced every day with fresh chemicals. Images were acquired using Zeiss Axiovert 200 fluorescent microscope equipped with Axiocam digital camera. Confocal Z-stack images were acquired using Olympus Fluoview FV1000.

Whole mount in situ hybridization (WISH)

WISH was performed with digoxigenin labeled antisense RNA probes for the following genes: *cp* (Korzh et al., 2001), *foxa3* (Field et al., 2003), *hhex* (Wallace et al., 2001), *hdac3* (gene accession number NM_200990.1), *gdf11* (gene accession number NM_212975), *prox1* (Liu et al., 2003), *insulin*, *elastase B* (Mudumana et al., 2004) according to the zebrafish book. The embryos were grown in 1-phenyl-2-thiourea (PTU) solution to block pigmentation.

HDAC enzymatic activity measurement

In order to measure the HDAC enzymatic activity in zebrafish embryos, protein extracts were isolated from wild type and VPA-treated embryos from a pool of about 100 embryos at required developmental stage using protein extraction reagent (Pierce, Rockford, IL) supplemented with protease inhibitor (Roche, Indianapolis, IN) and homogenized for 15 s (sigma ultra disintegrator). Samples were then centrifuged for 15 min at 10,000 rpm 4 °C. Clear supernatants were collected. HDAC fluorescent activity assay was performed according to the manufacturer's instructions using a unique substrate (Biomol, Plymouth Meeting, PA), which contains an acetylated lysine side chain. Fluor de Lys substrate was incubated with 20 μg of protein extract for 30 min at 37 °C, and the product produced was measured using SPECTRAmax GEMINI XS microplate spectrofluorometer with the SOFTMAX PRO V.3.1.2 system (Molecular Devices) with excitation at 355 nm and emission at 460 nm with a cut off filter of 455 nm. Assay was repeated thrice and the average arbitrary florescence units (AFU) were represented as total HDAC activity.

HDAC activity in the *hdac1* or *hdac3* morphants was similarly determined from embryos obtained from wild type fish and *Tg(lfabp:RFP; elaA:EGFP)*. Same amount of 5 bp mismatch morpholino injected embryos were used as control. In case of transgenic line, embryos were screened for liver defects based on the RFP expression, and protein extracts were collected from the pools of around 50 embryos at 3 dpf. To get rid of the background fluorescence activity from the transgenic embryos, fluorescence in the mismatch morpholino injected embryos was used to normalize the background fluorescence.

Real-time RT-PCR

Total RNA was extracted using RNAwiz™ (Ambion, USA). Real-time RT-PCR was performed using QuantiTect SYBR Green RT-PCR kit (Qiagen, USA) using Opticon 2 real-time PCR machine (MJ Research, USA) and analyzed using Opticon 2 software. Ct values were normalized against β-actin and fold

change in gene expression was calculated as described (Livak and Schmittgen, 2001). The primers used are: *gdf11*: Forward 5′ CGT CAT CAC AAT GGC TTC AGA, Reverse 5′ TTG AAG AAA CAA CAG GTC GGT TT.

Molecular cloning

Full length cDNAs for *hdac1* (NM_173236.1), *hdac3* (NM_200990.1) and *gdf11* (NM_212975) were obtained by high fidelity PCR using Advantage High Fidelity 2 (HF2) PCR kit (Clontech, USA) and a full length zebrafish embryonic cDNA library as template. The following sets of primers were used: *hdac1* Forward 5′-CGG GCA GGC GCA GGC TGT AAT T-3′, Reverse 5′-CAT GCA TCC AGG AGG ACT GGC-3′; *hdac3* Forward 5′-CGG CAA CAT GAC CAA TCG AAC TGC G T-3′, Reverse 5′-CGC TTT TAC CCA CAC ATC ACA GTC AAG-3′; *gdf11* Forward 5′-CGA TGA AAA GGT ATA ACT TTT A-3, Reverse 5′-CCA CTC TCC CCC CTC CCT TAC T-3′. The PCR products were cloned into pGEM-T easy vector (Promega) and confirmed by sequencing. For functional analysis, these genes were subcloned into pCS2 vector.

Gene knockdown by MO microinjection

MOs were purchased from Gene Tools (Philomatch, USA), and were diluted in sterile water at the concentration of 1 mM. They were designed to overlap the translational start site of the following genes: *hdac3* antisense 1: CATAGAAG-TACGCAGTTCGATTGGT, antisense 2: GCAGTTATTTCTAGCACGA-GAAAC, 5 bp mismatch control: CATAcAAcTACcCAGTTCcATTcGT; *hdac1* antisense: TTG TTC CTT GAG AAC TCA GCG CCA T, 5 bp mismatch control: TTc TTC CTT cAG AAg TCA cCG CgA T; *gdf11* antisense: ATA CCT TTT CAT GTT GTT AAA TAT C, 5 bp Mismatch: ATA gCT TTT gAT cTT cTT AAA aAT C and *vegf* antisense: GTATCAAATAAACAACCAAGTTCAT, 4 bp mismatch control: GTAaCAAtTAAACA ACCAtGTTgAT. For single knock-down, *hdac1* MO used is 3 or 6 ng/embryo and *hdac3* MO used is 12 ng/embryo. For double knockdown with *hdac1* and *hdac3*, both morpholinos were combined (*hdac1*, 3 ng/embryo; *hdac3*, 12 ng/embryo) and injected into 1–2 cell stage embryos. To rescue *hdac3* morphants (12 ng/embryo), zebrafish *gdf11* gene was co-knocked down by co-injecting *gdf11* MO (4 ng/embryo).

mRNA rescue and overexpression

To rescue the VPA-treated embryos, *hdac1* and *hdac3* 5′-capped mRNA was synthesized using m messenger m machine kit (Ambion, USA) and injected singularly or together into *Tg(lfabp:RFP; elaA:EGFP)* embryos at 1–2 cell stages. The injected embryos were raised to shield stage and divided into two groups, one group of embryos were then treated with VPA (10 μM) and the other group remained untreated control embryos. The embryos were raised to 5 dpf with fresh VPA in embryo water changed daily. To rescue VPA-treated embryos, *hdac1* mRNA (0.3 ng/embryo) and *hdac3* mRNA (0.3 ng/ml) were injected singularly or together. To rescue *gdf11* mRNA overexpression embryos (0.5 ng/embryo), *hdac3* mRNA (0.3 ng/embryo) was co-injected.

Results

HDACs are required for liver and exocrine pancreas formation in zebrafish

To investigate the role of HDACs in the organogenesis of liver/pancreas, we used valproic acid (VPA), a potent HDAC inhibitor which preferably inhibits class I HDACs, to treat zebrafish embryos at non-terotogenic concentrations (Pillai et al., 2004). Embryos from transgenic line *Tg(lfabp:RFP; elaA:EGFP)* which express RFP in liver (from 59–60 hpf onward) and GFP in exocrine pancreas (from 4 dpf onward) were treated with VPA (20 μM and 10 μM) from shield stage and the effects on liver formation were observed from 60 hpf onward. As shown in Fig. 1, in VPA-treated embryos, RFP could not be detected up to 4 dpf (~100% embryos, $n=320–350$) (Fig. 1a, panels A–F), suggesting the absence of liver in these embryos. RFP positive liver was only observed at 5 dpf, and the liver size is much smaller compared to control embryos at the same stage. Furthermore, liver remained the same size from 5 dpf to 8 dpf (data not shown). VPA interfered with liver formation in a dose-dependent manner. Under lower VPA concentrations (5 μM and 1 μM), RFP expression in liver could be observed at normal developmental stages (3 dpf), but the size of liver was much smaller ($n=250–300$) (data not shown). VPA also inhibited angiogenesis in zebrafish embryos, consistent with its anti-angiogenic activity reported earlier (Michaelis et al., 2004). The intersegmental vessels (ISVs) in the developing zebrafish embryos which are generated through angiogenesis either did not form or never connected to dorsal longitudinal anastamotic vessels (DLAVs) (Fig. 1a, compare panels G and H).

The effect of HDAC inhibition on liver formation was also confirmed by expression of *ceruloplasmin* (*Cp*), an early liver differentiation marker, by WISH. In VPA-treated embryos, *Cp* expression in liver was severely delayed, with no expression up to 72 hpf comparing to the normal expression which starts from 32 hpf (100% of embryos, $n=200$ embryos) (Fig. 1b, panels A–F). In contrast, Cp expression in YSL was not affected (Fig. 1B, panels D and F). At 4 dpf, a tiny *Cp* positive area was observed in about 30% ($n=200$) of VPA-treated embryos (Fig. 1B, panel H) whereas the majority (70%) of embryos still did not express *Cp*. At 5 dpf, *Cp* expression appeared in all VPA-treated embryos, but the liver was much smaller compared to untreated embryos at the same stage (Fig. 1b, panel J) (100% of embryos, $n=200$).

The formation of exocrine pancreas was also affected by VPA, with a delayed GFP expression in exocrine pancreas only observable at 5 dpf (100% embryos, $n=100$). The exocrine pancreas was also of much smaller size at this stage compared to control embryos (Fig. 1c, compare panels A vs. B and C vs. D). In contrast, development of endocrine pancreas marked by *insulin* (*ins*) expression from 2 dpf to 5 dpf was not affected by VPA (Fig. 1c, panels E–J) (100% embryos, $n=100$).

As earlier reports of the teratogenic effects of VPA on zebrafish embryos were observed at very high doses often in mM concentrations, we want to confirm the effectiveness of the low level VPA (20 μM) used in our experiments in inhibiting HDACs. Wild type embryos were treated with VPA and total HDAC enzymatic activity was measured from 15 somites to 5 dpf using a florescent based HDAC enzymatic activity assay (Fig. 2a). Total HDAC enzymatic activity in untreated embryos was found to gradually increase from 15-somite stage (about 16.5 hpf) and reached the highest level at 2 dpf and gradually decreasing from 3 dpf to 5 dpf. VPA at 20 μM effectively suppressed HDAC enzymatic activity at all the stages observed, with suppression of more than 75% at 2 dpf and 3 dpf (Fig. 2a). At 20 μM or lower, VPA is non-terotogenic in the first 3 days of embryonic development with no gross developmental deformities or retardation observed. However, from 3 dpf onward, small head and mild pericardia edema were observed, with morphological deformation more severe at later stages (Fig. S1).

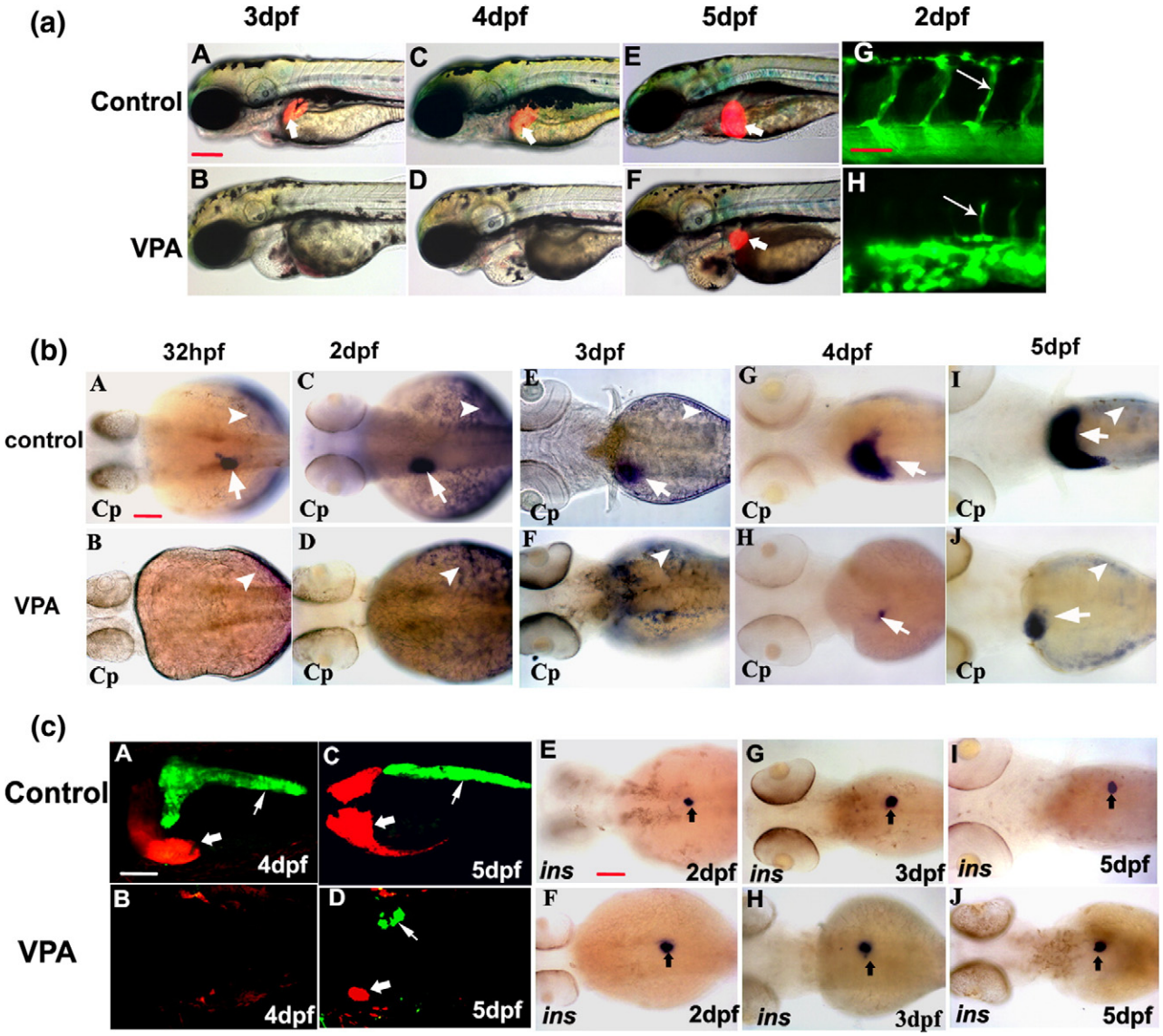

Fig. 1. HDACs are required for liver and exocrine but not endocrine pancreas formation. (a) Embryos from *Tg(lfabp:RFP; elaA:EGFP)* and *Tg(fli-1:EGFP)* were treated from shield stage with VPA (20 μM) as described in Materials and methods. Liver formation was examined by the appearance of red fluoresce (white arrows) at 3 dpf (A), 4 dpf (C) and 5 dpf (E and F). In VPA-treated embryos, liver was not formed up to 4 dpf as judged by the absence of red fluorescent, while a much smaller liver emerged at 5 dpf (E and F). Blood vessel was monitored by green fluorescence and ISV defect is indicated by thin white arrow (G, H). (b) Liver formation analyzed by liver differentiation marker *Ceruloplasmin* (*cp*) expression at various stages of liver formation including 32 hpf (A, B) and 48 hpf (C, D), 3 dpf (E, F), 4 dpf (G, H) and 5 dpf (I, J). *Cp* expression was absent in liver (white arrow) in VPA-treated embryos up to 3 dpf although its expression in YSL (white arrowhead) was not affected (C, D, E and F). A small number of liver cells start to express *Cp* at 4 dpf which grew, but never reached the control liver size at 5 dpf (I vs. J). All the images are dorsal views, anterior to the left. (c) Liver and exocrine pancreas formation analyzed in transgenic line and endocrine pancreas formation analyzed by insulin expression. Panels A–D are merged images of z-stack taken by confocal microscope. Liver (in red) is indicated by a thick white arrow and exocrine pancreas (in green) by a thin white arrow. Endocrine pancreas (black arrow, E–J) as indicated by *insulin* (*ins*) expression was not affected by VPA treatment from 2 dpf to 5 dpf. All the images are dorsal views, anterior to the left. Scale bar represents 100 μm for all panels except in panel aG, which represent 30 μm and panel cA, which represents 50 μm.

To confirm that inhibition of HDACs is responsible for liver defects observed in VPA-treated embryos, embryos were treated with a structurally unrelated HDAC inhibitor TSA which inhibits both Class I and II HDACs (Pillai et al., 2004), as well as Valpromide (VPM), a structural analogue of VPA which does not inhibit HDAC. Liver formation and growth were not affected in embryos treated with VPM at all the stages observed (Fig. 2b, panels C, E and H), whereas liver formation and growth were inhibited in embryos treated with TSA (Fig. 2b, panels B, D and G). Similar to VPA, TSA treatment leads to delay of RFP appearance in liver until 5 dpf and a much smaller liver was observed compared to control. We therefore concluded that liver defects in VPA-treated embryos were due to inhibition of HDACs. HDAC(s) are required for organogenesis of liver and exocrine pancreas but not endocrine pancreas in zebrafish.

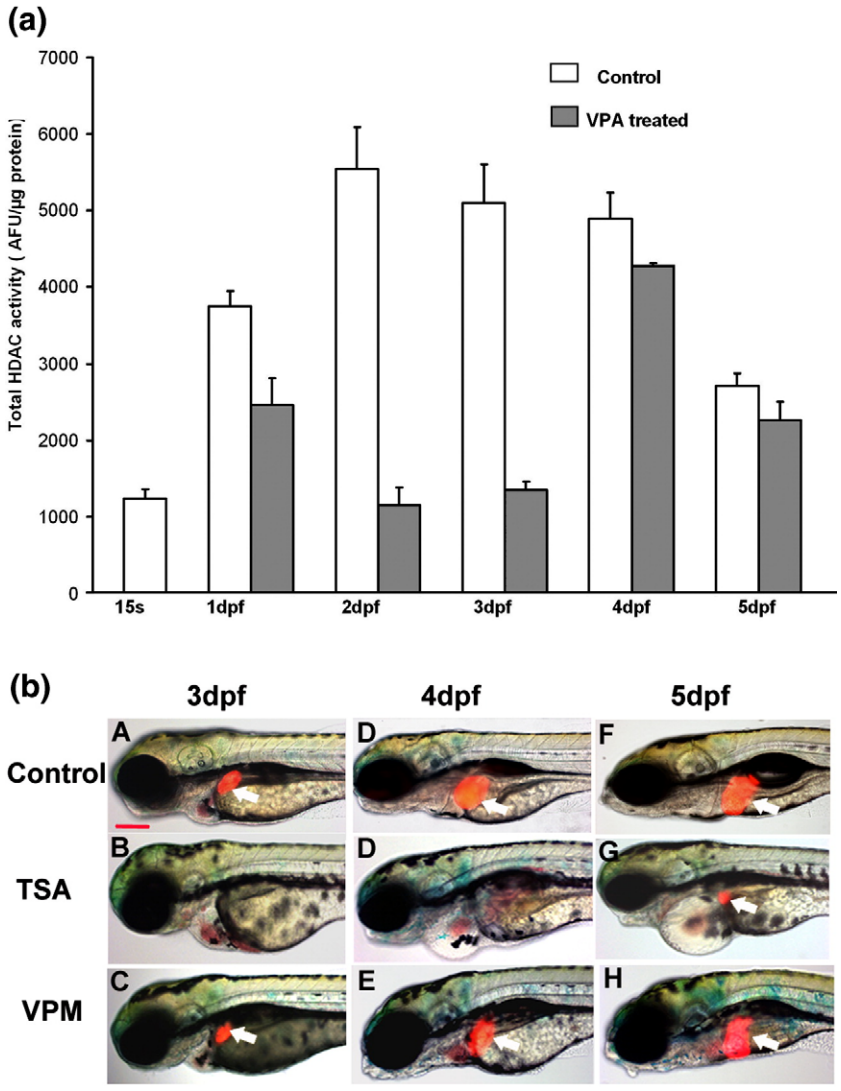

Fig. 2. The liver defects in VPA-treated embryos correlated with inhibition in HDAC enzymatic activity. (a) HDAC enzymatic activity in zebrafish embryos were measured by fluorescent based assay. Embryos were treated (from 15-somite stage) with VPA (20 μM) and harvested at different stages. Total HDAC enzymatic activity was inhibited from 1 dpf onward and maximum reduction (around 75%) was observed at 2–3 dpf in VPA-treated embryos. (b) Embryos from *Tg(lfabp:RFP; elaA:EGFP)* were treated with TSA (B, D, G), a structurally unrelated HDAC inhibitor, and Valpromide (VPM) (C, E, H), a structural analogue of VPA which does not inhibit HDAC. Liver formation was observed at 3 dpf (A–C), 4 dpf (D–E) and 5 dpf (F–H). No liver was observed in TSA-treated embryos up to 4 dpf (B, D) while a small liver appeared at 5dpf (G, white arrow). Liver formation was unaffected in VPM-treated embryos (C–H, white arrows). All the images are lateral view, anterior to the left. Scale bar is 50 μm.

The liver defects in VPA-treated embryos were not due to inhibition of angiogenesis

Since angiogenesis inhibition in vitro by VPA is preceded by histone hyperacetylation (Michaelis et al., 2004), it is possible that the delay in liver formation is an indirect result of the blood vessel defect. In addition, VPA suppresses the expression of vascular endothelial growth factor (VEGF) in cultured cancer cells, a key angiogenic growth factor regulating embryonic vascular development in zebrafish (Liang et al., 2001; Nasevicius et al., 2000; Zgouras et al., 2004). Indeed, VPA also inhibited VEGF production at both mRNA and protein levels in zebrafish embryos (data not shown). While vascularization is essential for liver formation in mouse (Zaret, 2002), it is not clear if a similar requirement also occurs in zebrafish. Earlier report of normal liver budding in the zebrafish mutant *cloche* which lacks most of the endothelial and hematopoietic lineages suggests that vascularization may not be required in zebrafish liver formation (Field et al., 2003; Liao et al., 1997; Stainier et al., 1995).

To clarify this, specific angiogenesis inhibitors SU5614 and SU1498 were used to inhibit angiogenesis and their effects on liver formation were analyzed; both SU5614 and SU1498 are known to inhibit VEGFR1/Flk-1 tyrosine kinase signaling (Mendel et al., 2000). In order to observe the angiogenesis defects and liver formation in the same embryo, *Tg(fli-1:EGFP)* (Lawson and Weinstein, 2002), which expresses GFP in blood vessels, was crossed with *Tg(lfabp:RFP, elaA:EGFP)*, and embryos were screened for homozygous expression of all three transgenes and stable line was generated and herein will be

called triple transgenic line and used in the following experiment.

In zebrafish, the subintestinal vein (SIV) branches to hepatic portal vein around 72 hpf, penetrates and vascularizes liver at this stage (Isogai et al., 2001) (Figs. 3A–D). At 5 dpf, a highly vascularized liver can be seen in control embryos (Fig. 3D). In VPA-treated embryos, SIV was never formed during the observation period (up to 8 dpf). At 5 dpf, blood vessels were substantially reduced or absent in liver (Fig. 3H) and the size of liver was significantly reduced. Blood circulation in treated embryos was normal up to 3 dpf, but circulation becomes slower at 4 dpf and was completely undetectable from 5 dpf onward with obvious cardiac edema (Fig. 3 and data not shown).

Both SU5614 and SU1498 (5 μM) inhibited angiogenesis with ISVs either did not form or formed abnormally (Figs. 3I and M). At 3 dpf, SIV was either absent or defective in treated embryos. However, not only was normal liver observed in these embryos at 3 dpf, but it also grew bigger from 3 dpf to 5 dpf despite the abnormal shape of the embryo (Figs. 3I–P). Similar phenotypes were also observed in two other angiogenesis inhibitors (2-methoxyestradiol and Genestein) treated embryos (data not shown). In addition, zebrafish *vegf* gene was knocked down by MO microinjection and liver formation is also generally normal in *vegf* morphants (data not shown; Liang et al., 2001; Nasevicius et al., 2000). The levels of angiogenesis inhibition judged by ISV abnormality by these chemical inhibitors were similar to that of VPA. It is noted that blood circulation was normal up to 3 dpf in chemical-treated embryos (data not shown). Altogether, these results demonstrate that the liver defects induced by HDAC inhibitors are most likely results of reduced HDAC activity rather than defective vascularization. Liver development and growth in zebrafish do not seem to depend on liver vascularization.

HDACs are required for early liver formation

In zebrafish, liver and posterior pancreas bud emerges from the anterior gut endoderm around 24–28 hpf and liver development involves multiple stages including specification, budding, differentiation and growth. To determine which stage (s) HDAC function is critically important, embryos were treated with VPA for short and defined intervals at different developmental stages crucial for liver formation and compared with embryos under VPA continuously. In addition to observe liver phenotype in *Tg(lfabp:RFP; elaA:EGFP)*, expression of hepatoblast markers *hhex* and *prox1*, endoderm marker *foxa3* and liver differentiation marker *Cp* were also investigated.

We noted that the delay in liver appearance in VPA-treated *Tg(lfabp:RFP; elaA:EGFP)* embryos depended on the developmental stages the treatment was initiated (Table 1A). Delays in liver formation in this transgenic line were observed only when VPA treatment was initiated between shield to 15-somites stage (6 hpf to 16 hpf) (Table 1A and data not shown). A short

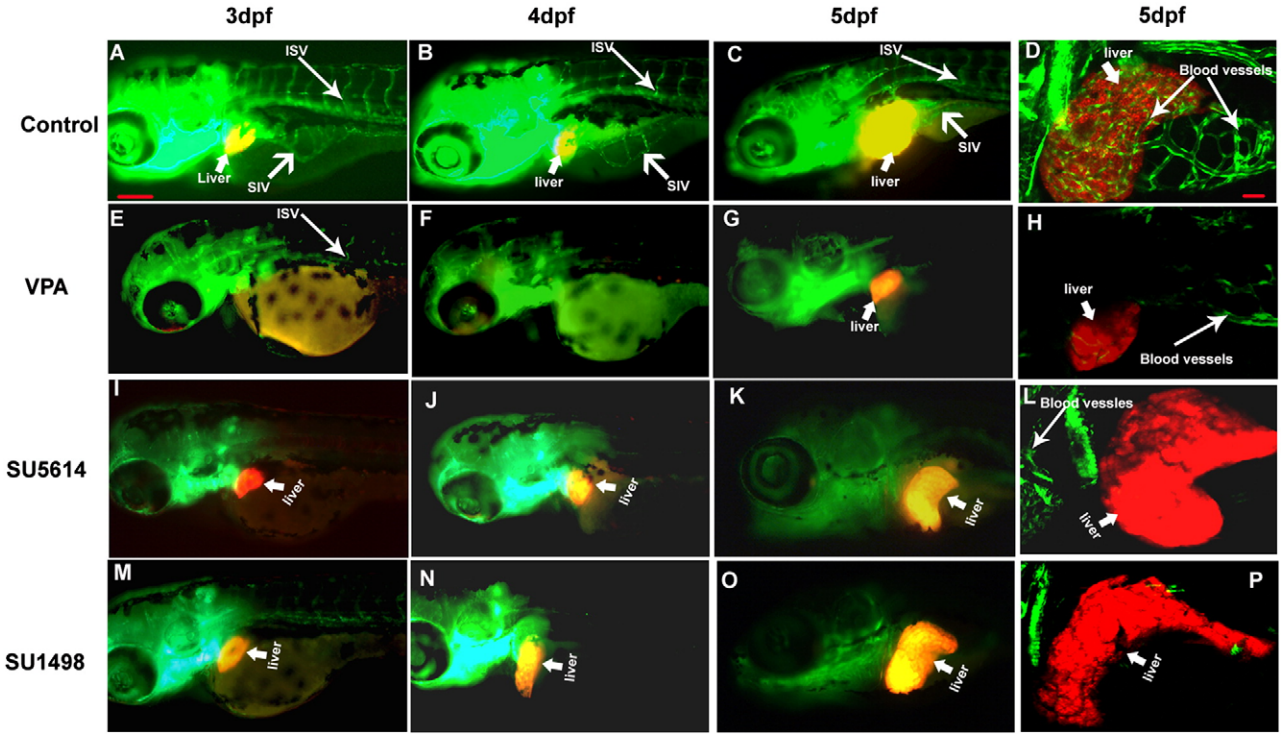

Fig. 3. Liver formation in zebrafish does not require vascularization. Zebrafish embryos from triple transgenic line were treated with VPA (20 μM). Severe defects in intersomatic blood vessels (ISV) (thin white arrows) and subintestinal blood vessels (SIV) (wide white arrow) were observed up to 5 dpf (E–H). Liver only appeared on 5 dpf and no or minimum liver vascularization was observed (H). Similar angiogenesis defects were observed in embryos treated with angiogenesis inhibitors SU5614 (5 μM, I–L) and SU1498 (5 μM, M–P). However, liver (thick white arrows) formed normally on 3 dpf and grew extensively from 3 dpf to 5dpf in these embryos (I–P). All images are lateral view, anterior toward left. The images D, H, L and P are confocal images of merged z-stacks. The scale bar is 100 μm in panel A, and 30 μm in panel D.

Table 1A
Summary of the effect of VPA treatment time on liver formation in *Tg(lfabp: RFP; elaA:EGFP)* zebrafish embryos

Treatment start time	Treatment end time	No. of embryos	Liver in *Tg(lfabp:RFP; elaA:EGFP)*
–	–	>500, $n=5$	Liver appears at 3 dpf, grows larger to 5 dpf,
6 hpf	5 dpf	350, $n=5$	Delayed appearance, no liver up to 4 dpf, small liver at 5 dpf
6 hpf	18 hpf	200, $n=2$	Delayed appearance, no liver at 3 dpf, small liver at 4 dpf, remain small to 5 dpf
24 hpf	5 dpf	200, $n=2$	Small liver at 3 dpf, remained small to 5 dpf
24 hpf	48 hpf	200, $n=2$	Small liver at 3 dpf, remained small to 5 dpf
48 hpf	5 dpf	200, $n=2$	Small liver at 3 dpf, remained small to 5 dpf
48 hpf	3 dpf	200, $n=2$	Small liver at 3 dpf, remained small to 5 dpf
3 dpf	5 dpf	100, $n=2$	Liver appears at 3 dpf, grows larger to 5 dpf, similar to untreated embryos
3 dpf	4 dpf	100, $n=2$	Liver appears at 3 dpf, grows larger to 5 dpf, similar to untreated embryos

RFP positive liver can readily be observed at 3 dpf from this line. "*n*" indicates number of experimental repeats. For short period treatment, VPA (20 μM) was removed after 12 or 24 h of treatment and embryos were grown in normal embryo water up to 5 dpf. "–": not applicable.

and transient VPA treatment from 6 hpf to 18 hpf also leads to a delay in liver appearance with a small liver first appearing at 4 dpf and remained small up to 5 dpf. If VPA treatment started from 24 hpf or later and continued to 5 dpf, a small RFP+ liver appeared at the normal developmental tempo at 3 dpf. Transient VPA treatment from 24 to 48 hpf or from 48 hpf to 3 dpf also both lead to appearance of small RFP+ liver (*lfabp* expression) at 3 dpf. Interestingly, even though VPA is removed after treatment, liver remained small up to 5 dpf (Table 1A). When VPA is present from 3 dpf to 4 dpf, liver developed normally and grew larger between 3 dpf and 5 dpf (Table 1A). These results indicate that VPA inhibits early liver formation when present during 6–18 hpf, and causing a delay in liver development. HDACs are most likely required in the specification of liver primordium before liver buds from endoderm. When present from 3 dpf onward, VPA does not inhibit liver growth and expansion.

When VPA is present continuously from shield stage (6 hpf), *hhex* expression at 24 hpf was absent in liver (thick white arrow) and pancreas (thick black arrow) regions (Fig. 4A vs. C; Table 1B) whereas its expressions in intermediate cell mass (ICM) (Fig. 4A vs. C, thin black arrow) and notochord (A–D, white arrowhead) were not affected (100% embryos, $n=150$). Under VPA, *hhex* expression was observed in the anterior endoderm at this stage (C and D, black arrowhead). Similarly, at 28–30 hpf, *prox1* expression was absent in liver region (Fig. 4E vs. G and F vs. H, thick white arrow) in VPA-treated embryos whereas its expressions in lens (E and F) and neurotube (F and H, thin white arrow) were not affected (100% of embryos, $n=\sim 100$). *foxa3* expression at 28–30 hpf showed that endoderm thickening in liver region failed to occur in VPA-treated embryos, suggesting a delay of liver budding (Fig. 4I vs. J, thick white arrow; Table 1B). Meanwhile, *foxa3*'s expression in anterior intestine was unaffected (Fig. 4J). At 48 hpf, expressions of *hhex* and *prox1* both showed a significantly reduced liver and pancreas (Fig. 4K vs. L, M vs. N, and Table 1B, 100% of embryos, $n=100$). However, *foxa3* expression clearly showed that liver and pancreas have budded by 48 hpf (Figs. 4O and P), indicating that liver budding, although delayed, can still occur under VPA. Interestingly, at 48 hpf, the liver size reduction in VPA-treated embryos revealed by *foxa3* expression was smaller than that revealed by *hhex* or *prox1* expression (Fig. 4O vs. P, compare to K vs. L and M vs. N; $n=100$). Therefore, not all *foxa3* positive liver cells have become hepatoblasts that express *hhex* and *prox1* in VPA-treated embryos at this stage. In addition, hepatic duct (the furrow between liver bud and the adjacent esophagus, thin green arrow) was not obvious and swim bladder was not visible under VPA (Fig. 4O vs. P). Furthermore, hepatoblasts differentiation into hepatocytes has yet to occur as the liver differentiation marker *Cp* was not expressed in liver until 4 dpf under continuous VPA (Fig. 1B and Table 1B). These results show that endoderm cells remain competent to become hepatoblasts and bud to form liver after 28 hpf and hepatoblasts remain competent to differentiate into hepatocytes after 4 dpf, consistent with earlier reports (Shin et al., 2007).

When VPA was transiently present from 6 to 24 hpf, 50% of embryos have no *hhex* expression at 32 hpf and 0% embryos have *Cp* expression (Table 1B). HDACs are therefore crucial for liver specification from endoderm. Transient VPA treatment from 6 to 18 hpf which led to delay in *lfabp* expression (liver only appeared at 4 dpf) in transgenic line also supported a role of HDACs in inhibiting hepatoblast specification from endoderm cells (Table 1A). It seems that hepatoblast determination occurs much earlier than the initial appearance of liver primordium from 24 hpf. This is consistent with the finding that Bmp and Fgf signaling is required for liver specification from 18 to 24 hpf (Shin et al., 2007).

When VPA was present from 24 to 36 hpf transiently (hepatoblast already specified), *Cp* expression was absent in 70% of embryos at 48 hpf, indicating suppression of hepatoblast differentiation to hepatocyte. In addition, in the 30% embryos that do expression *Cp*, Cp+ liver is much smaller (Table 1B). In contrast, liver size is nearly normal judged by *prox1* and *hhex* expression. These results clearly show that VPA inhibits hepatoblast differentiation to hepatocyte after 24 hpf.

When VPA is present transiently from 48 hpf to 60 hpf, Cp+ liver is also small at 3 dpf (Table 1B). It seems that when hepatocyte already differentiated to certain extent at 48 hpf and is Cp+, subsequent presence of VPA suppressed either additional hepatoblast differentiation to hepatocyte or proliferation of Cp+ hepatocyte or both, leading to a small Cp+ liver phenotype at 3 dpf.

All together, the above results clearly show that VPA inhibited primarily early liver formation including specification, budding and differentiation, but most likely not hepatocyte proliferation. However, the possibility that VPA also inhibited

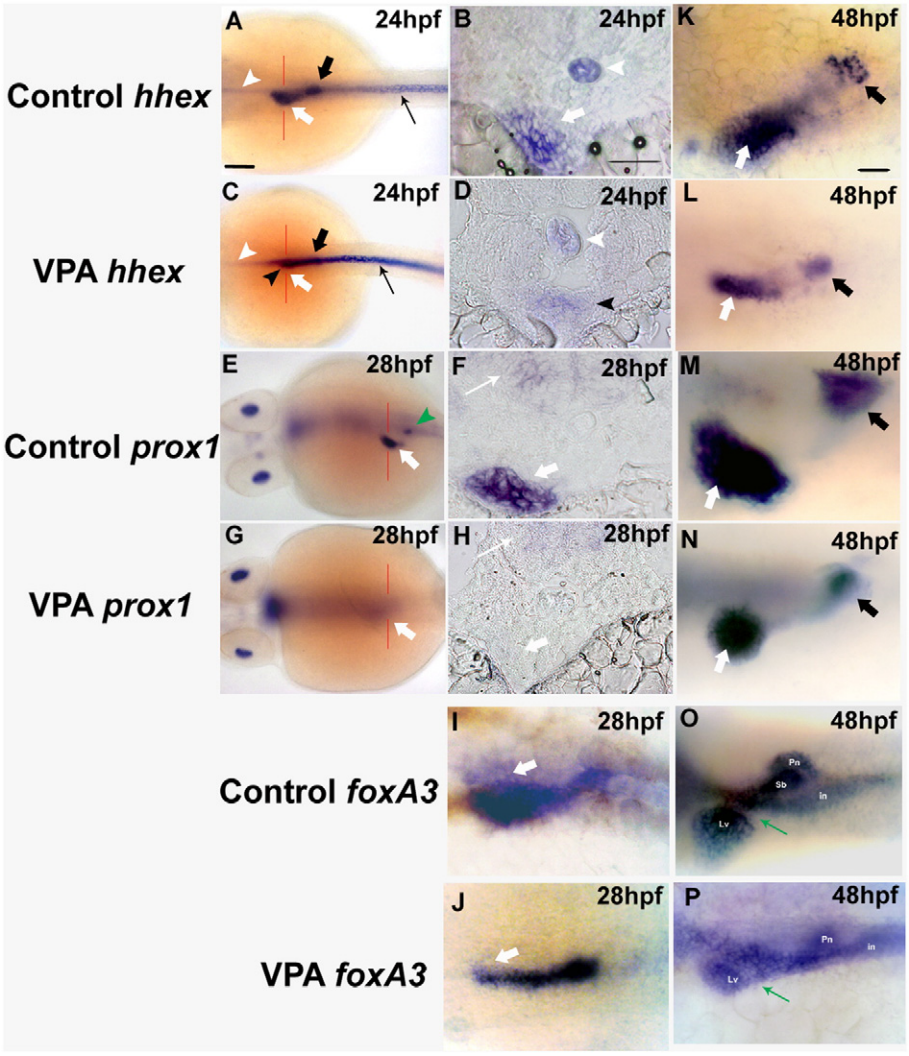

Fig. 4. HDACs are required for early liver development. Expressions of early liver markers were analyzed by WISH in WT and VPA-treated embryos including *hhex* (A–D, K, L), *prox1* (E–H, M, N) and *foxa3* (I, J, O, P). All panels are whole mount pictures except panels B, D, F and H which are tissue sections corresponding to panels A, C, E and G, respectively, with section planes indicated by red lines. In all panels, liver is indicated by a thick white arrow while pancreas is indicated by a thick black arrow. Expression of *hhex* was completely abolished in liver and pancreatic islet (C vs. A) at 24 hpf in VPA-treated embryos while its expression in intermediate cell mass (ICM) (A vs. C, thin black arrow) remains unaffected. Note that panels A and C were focused on different focal planes with panel A focusing on the liver region while panel C focusing on the more posterior ICM. White arrowhead indicates *hhex* expression in notochord (A–D) and black arrowhead in panels C and D refers to *hhex* expression in anterior endoderm. At 48 hpf, *hhex* expression in liver and pancreatic islet was significantly reduced (K vs. L). *prox1* expression in liver region was absent in treated embryos at 28–30 hpf (E vs. G, F vs. H) while its expression was greatly reduced at 48 hpf (M vs. N). The green arrowhead in panel E indicates interregnal gland which also expresses *prox1* at this stage. Initial endoderm thickening at liver region was absent in treated embryos at 28–30 hpf as judged by *foxa3* expression (I vs. J, white arrow). At 48 hpf, a slightly small and compressed liver was observed in VPA-treated embryos while the hepatic duct was still not well formed (O vs. P, thin green arrow). All imagines are dorsal view, anterior to the left. Scale bar represents 100 μm in panels A, C, E, G, I and J; 20 μm in panels B, D, F and H; 50 μm in panels K–P. Lv: liver; Pn: pancreas; in: intestine; Sb: swim bladder.

hepatocyte proliferation during the initial liver expansion phase at 2–3 dpf cannot be completely ruled out at this moment. These results demonstrate the importance of HDACs in early liver development and show that short period VPA treatment generated a long lasting inhibitory effect on subsequent liver development.

hdac1 has a general role in zebrafish development including liver and pancreas formation

In mammals, HDACs are a large gene family with 4 members in class I subfamily identified so far (Marks et al., 2003). As VPA inhibits multiple HDACs, it is important to determine which HDAC plays a dominant role in zebrafish liver formation. Two zebrafish class I HDAC cDNA sequences (*hdac1* and *hdac3*) were available from Genbank at the time of our study. In VPA-treated embryos, both *hdac1* and *hdac3* mRNAs were down-regulated as determined by qRT-PCR (data not shown). We therefore set out to investigate the role of these two *hdacs* in zebrafish liver formation. Knockdown of each of the two *hdacs* by antisense MO injection (6 ng/embryo *hdac1* MO and 12 ng/embryo *hdac3* MO) effectively inhibited total HDAC activity in embryos, with *hdac1* knockdown more effective (up to 75% HDAC activity inhibited), indicating the

Table 1B
Summary of the effect of VPA treatment time on liver marker expression

Treatment start time	Treatment end time	Embryo stage for WISH	Liver marker expression [% embryos] (liver size)		
			prox1+	*hhex+*	*cp+*
6 hpf	24 hpf	24 hpf	–	0%	–
6 hpf	28–30 hpf	28 hpf	0%	ND	–
6 hpf	32 hpf	32 hpf	ND	ND	0%
6 hpf	48 hpf	48 hpf	100% (small)	100% (small)	0%
6 hpf	3 dpf	3 dpf	ND	ND	0%
6 hpf	4 dpf	4 dpf	ND	ND	100% (small)
6 hpf	24 hpf	32 hpf	100% (small)	50% (small)	0%
24 hpf	36 hpf	48 hpf	100% (marginal small)	100% (marginal small)	30% (small)
48 hpf	60 hpf	3 dpf	ND	ND	100% (small)

ND: not determined. "–": not applicable. Number of embryos in each treatment is 30–150. VPA used is 20 μM.

main contribution of *hdac1* toward the total HDAC activity in zebrafish embryos (Fig. 5).

Zebrafish *hdac1* mutant has been isolated and is embryonic lethal. *hdac1* is required for neuronal specification during zebrafish CNS development (Cunliffe, 2004; Cunliffe and Casaccia-Bonnefil, 2006), craniofacial cartilage development (Pillai et al., 2004), and retinal neurogenesis (Yamaguchi et al., 2005). However, the role of *hdac3* in zebrafish development has not been investigated.

Each gene was individually knocked down in *Tg(lfabp:RFP; elaA:EGFP)* by antisense MO. As shown in Fig. 6a, *hdac1* morphants showed similar phenotype as *hdac1* mutants reported earlier with curved body, smaller head, craniofacial and eye defect as well as severe cardiac edema (Fig. 6a, panels B and D). The 5 bp mismatch mutant MO (control) at the same concentration did not produce any of these defects (Fig. 6a, panels A and C). At 3 dpf, RFP+ liver was observed in *hdac1* morphants (70% of injected embryos, $n=150$), with certain embryos showing a somewhat smaller liver (Fig. 6a, panel B and Fig. 9C). However, liver failed to grow to the same size from 3 dpf to 5 dpf compared to control embryos (Fig. 6a, panels B, F and H). At the MO dose of 6 ng/embryo, most of the embryos could develop and survive until 4–5 dpf. Morphants developed at normal pace up to 48 hpf, but subsequent development was delayed for up to 24 h compared to control. ISV was only minimally affected in these morphants as observed in *Tg(fli-1:EGFP)*, but SIV was not formed (Fig. 6a, panel D; 40% of injected embryos, $n=100$). Morphants have no blood circulation and severe edema formed from 3 dpf onward, making live fluorescent imaging in the transgenic line very difficult. We therefore analyzed exocrine pancreas development by *elaB* expression using WISH. As shown in Fig. 6b, exocrine pancreas was also severely suppressed in *hdac1* morphants while the endocrine pancreas shown by insulin expression was not affected at all the stages observed (Fig. 6b, panels D, F and H). These morphants could not survive beyond 5 dpf. Higher amount of *hdac1* MO killed the embryos at earlier stages.

Therefore, it seems that *hdac1* is a crucial gene that plays a global and general role in zebrafish embryonic development and knockdown of *hadc1* generated severe embryonic defects and high amount of MO leads to death of the embryos at early developmental stages. In addition to liver and exocrine pancreas formation, *hadc1* is also critical for neurogenesis, eye

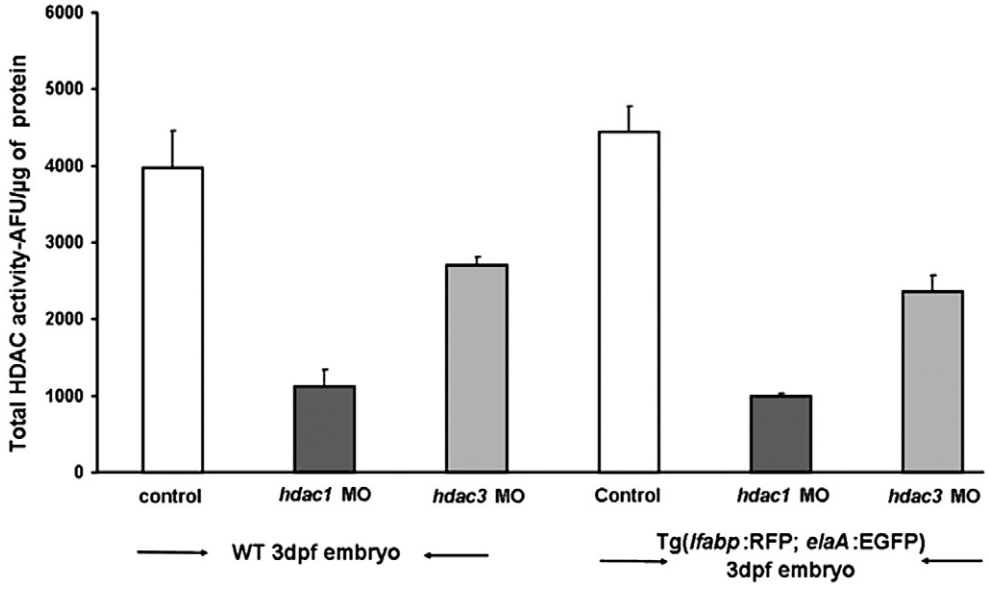

Fig. 5. *hdac1* is responsible for the majority of HDAC enzymatic activity compared to *hdac3* in zebrafish embryos. To check the effectiveness of knocking-down individual HDAC with antisense morpholino, total HDAC enzymatic activity was measured by the fluorescent based HDAC enzymatic activity at 3 dpf. *hdac1* morphants showed a dramatic reduction in total HDAC enzymatic activity with almost 75% of HDAC activity suppressed while *hdac3* morphants only showed about 25–30% reduction compared to 5 bp mismatch morpholino injected embryos in both WT and *Tg(lfabp: RFP; elaA:EGFP)* background. HDAC activity is indicated by artificial fluorescent unit (AFU)/μg of total embryo protein.

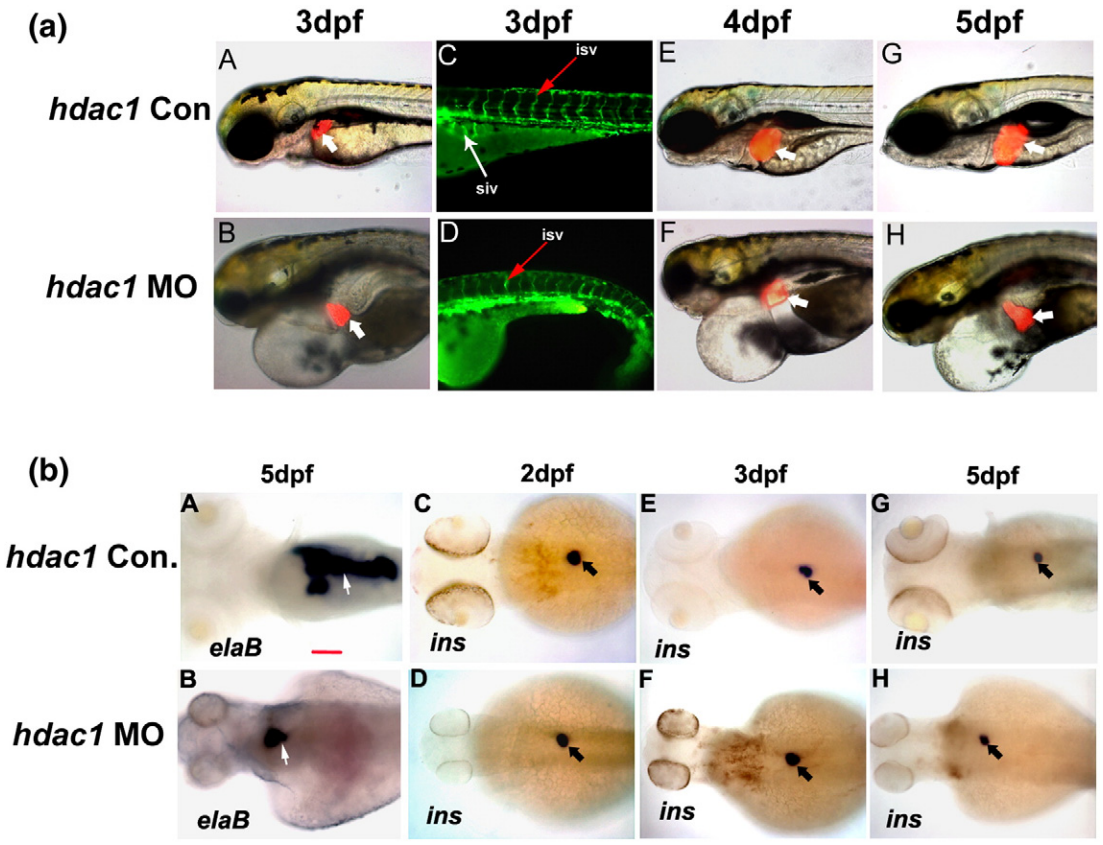

Fig. 6. Role of *hdac1* in zebrafish liver, pancreas and blood vessels development. (a) Liver development in *hdac1* morphants (6 ng/embryo MO) was analyzed in *Tg (lfabp:RFP; elaA:EGFP)* from 3 dpf to 5 dpf. Control embryos were injected with the same amount of *hdac1* 5 bp mismatch MO. Liver (thick white arrow) formed relatively normal in *hdac1* morphants at 3 dpf (A, B). However, its subsequent growth was reduced compared to control embryos (E–H). Angiogenesis was analyzed in *Tg(fli-1:EGFP)* at 3 dpf. SIVs were absent (thin white arrow, D) while ISV defects were mild and rare (thin red arrow, C and D). *hdac1* morphants exhibited global embryonic defects with severe cardiac edema, small head and eyes as well as absence of craniofacial cartilage structures (B–H). Scale bar is 100 μm. (b) Zebrafish pancreas development in *hdac1* morphants was analyzed by *elastase B* (A, B) and *insulin* (C–H) expression through WISH in *hdac1* morphants with 5 bp mismatch MO injected embryos as control (Con.). Exocrine pancreas (white arrow) was significantly reduced at 5 dpf (A, B) but endocrine pancreas formation (black arrow) was not affected (C–H). All images are dorsal views, anterior to the left. Scale bar is 100 μm.

formation, head and pharyngeal arch development, as well as angiogenesis.

hdac3 is specifically required for liver development in zebrafish

In contrast to *hdac1* morphants, *hdac3* morphants presented normal head and body shape with no cardiac edema at 3 dpf (even with up to 4 times more MO injected comparing to *hdac1* morphants). A smaller liver appeared at 3 dpf (Fig. 7a, panel B), and it grew somewhat subsequently up to 5 dpf but remained smaller comparing to control, resembling low concentration VPA treatment (5 μM or 1 μM) (Fig. 7a, panel B, F and H). Similar to VPA treatment, liver size was reduced about 50% in *hdac3* morphants at 5 dpf as determined by the total number of liver cells (Fig. S2). Angiogenesis defects were obvious, and dose-dependent on the amount of *hdac3* MO injected (Fig. 7a, panel D). A second *hdac3* MO targeting the 5′-UTR also showed similar dose-dependent defects on liver development, confirming the role of *hdac3* in liver growth (data not shown). Blood circulation was normal up to 3 dpf but became slower by 5 dpf. A mild cardiac edema appeared on 4 dpf (Fig. 7a). Heart presented a thin tube shape without looping at 5 dpf (data not shown).

The liver defects in *hdac3* morphants observed in *Tg(lfabp: RFP, elaA:EGFP)* were verified by *Cp* expression. As shown in Fig. 7b, *Cp* expression in *hdac3* morphants was absent in the liver region at 32 hpf and 48 hpf (white arrow) whereas its expression in YSL was not affected (white arrowhead). *Cp* expression in liver starts from 3 dpf in morphants, but its expression was reduced compared to control embryos from 3 dpf to 5 dpf (Fig. 7b, panels F and H). Surprisingly, both exocrine and endocrine pancreas formation and growth were not affected in *hdac3* morphants as shown by *elaA*:EGFP expression in transgenic line, and *elastase B* expression in WT embryos for exocrine pancreas (Fig. 7c, panel D) and insulin expression for endocrine pancreas (Fig. 7c, panels F, H and J). These results indicate that *hdac3* is specifically required for liver formation.

To analyze the role of *hdac3* in early liver formation, expression of early liver markers *hhex*, *prox1* and *foxa3* was analyzed in *hdac3* morphants. Expression of *hhex* in our local wild type embryos was first detected at about 24 hpf. Reduced *hhex* expression was observed in liver region of *hdac3* morphants at 28–30 hpf and 48 hpf (40–50% of morphants, $n=150$) (Fig. 8A vs. B, C vs. D) (white arrow), whereas *hhex*

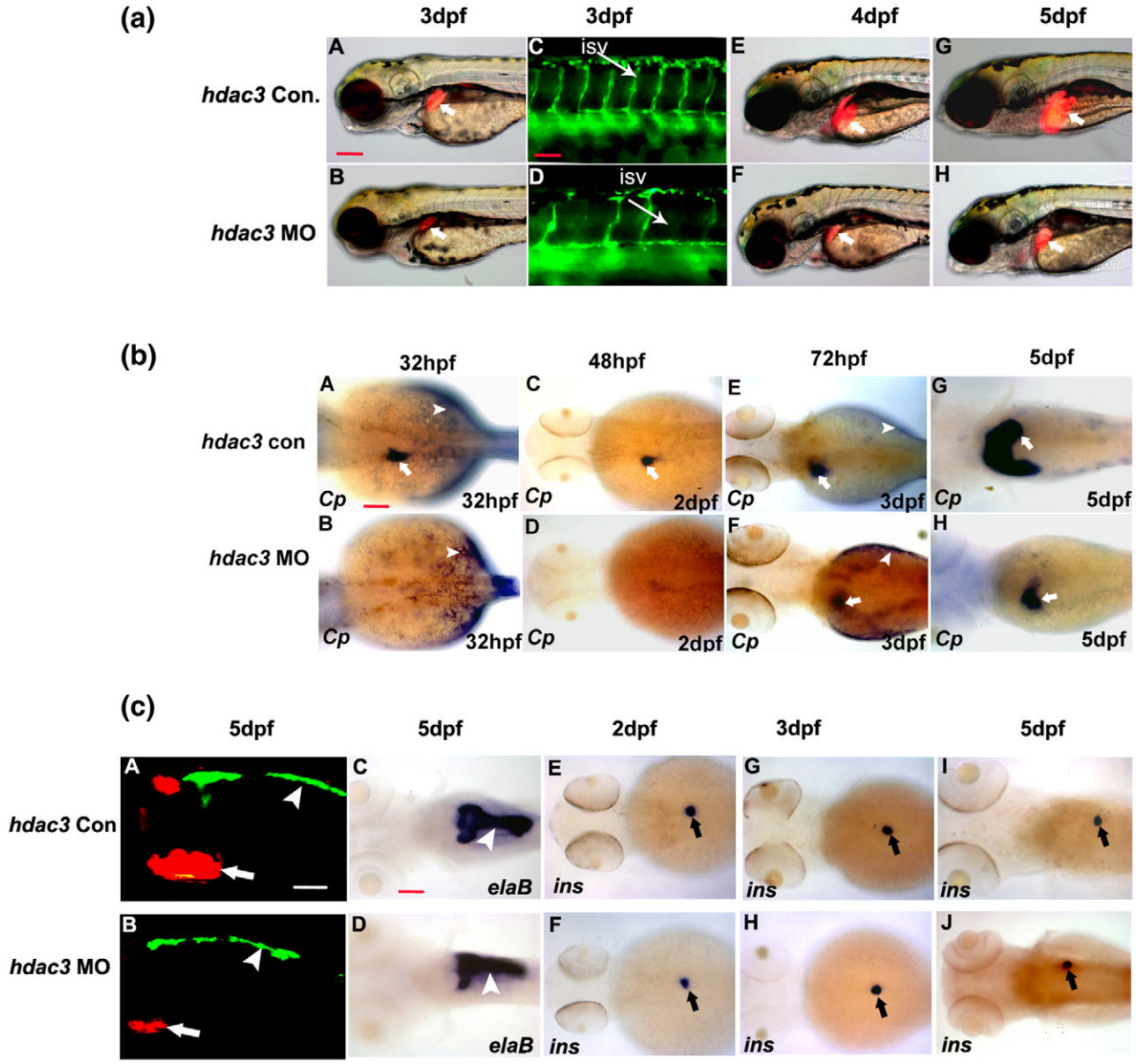

Fig. 7. *hdac3* is specifically required for liver formation in zebrafish. (a) *hdac3* was knocked down by antisense morpholino (12 ng/embryo) in *Tg(lfabp:RFP; elaA:EGFP)* and liver formation was observed from 3 dpf to 5 dpf. Control (Con.) embryos were injected with 5 bp mismatch antisense morpholino. Blood vessels formation was monitored in *Tg(fli-1:EGFP)* at 3 dpf. Liver (thick white arrow) was present at 3 dpf, but its size is much smaller (A vs. B). In addition, it failed to grow from 3 dpf to 5 dpf or reduced growth was observed compared to control embryos (E–H). ISV (thin white arrow) was disrupted. All the images are lateral view, anterior to the left. Scale bar represents 100 μm for all panels except panels C and D which is 50 μm. (b) Liver formation in *hdac3* morphants monitored by WISH with liver marker *Ceruloplasmin* (*Cp*) at 32 hpf (A, B), 2 dpf (C, D), 3 dpf (E, F) and 5 dpf (G, H). In *hdac3* morphants, *Cp* expression (white arrow) was absent up to 2 dpf (A, D) whereas a reduced liver was observed at 3 dpf (E, F) and 5 dpf (G, H). All images are dorsal view, anterior to the left. Arrowhead indicates *Cp* expression in YSL. (c) *hdac3* is not involved in pancreas formation. Exocrine and endocrine pancreas were monitored by GFP in *Tg(lfabp:RFP; elaA:EGFP)* and WISH with insulin, respectively. Control embryos were injected with same amount of 5 bp mismatch morpholino. Both exocrine pancreas (white arrowhead, A–D) and endocrine pancreas (black arrow, E–J) were not affected in *hdac3* morphants, whereas liver (red fluorescence, white arrow) was affected (A vs. B). All the images are dorsal view, anterior to left. Scale bar is 50 μm.

expression in pancreatic islet was less affected (Fig. 8C vs. D, black arrow). *prox1* expression also showed a reduced liver in *hdac3* morphants, although the liver defect is milder than that of VPA-treated embryos (Fig. 8E vs. F, G vs. H, 50% of morphants, $n=100$). Anterior endoderm thickening in liver region (white arrow) which represents the initial stage of liver budding was absent at 28–30 hpf as indicated by *foxa3* expression (Fig. 8I vs. J, 40% of morphants, $n=200$) while the anterior intestinal expression was not affected. These results indicate that at 28–30 hpf, fewer hepatoblasts formed from endoderm in *hdac3* morphants. In addition, although liver primordium exists (*hhex+prox1+*) and anterior endoderm looping occurred, liver budding is delayed in these morphants. At 48 hpf, *foxa3* expression indicated that liver has budded from endoderm, although it is slightly smaller (Fig. 8K vs. L, 40% of morphants, $n=200$). Swim bladder was absent at this

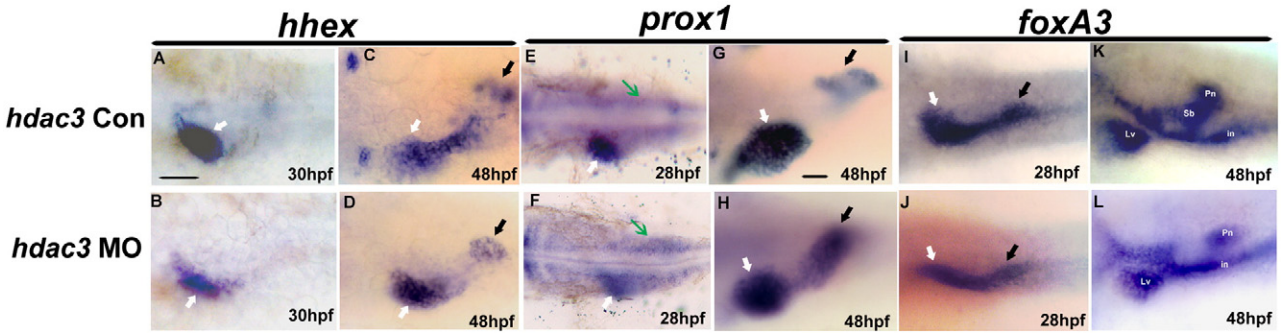

Fig. 8. *hdac3* is required for early liver formation. WISH with three hepatoblast markers *hhex* (A–D), *prox1* (E–H) and *foxa3* (I–L) was analyzed in *hdac3* morphants. At 28–30 hpf, *hhex* expression in liver (white arrow) was greatly reduced in *hdac3* morphants (A vs. B). It remained reduced at 48 hpf (C vs. D) whereas its expression in pancreatic islet (black arrow) was less affected. *prox1* expression was reduced in liver region at 28–30 hpf (white arrow, E vs. F) and at 48 hpf (G vs. H), while its expression in mesoderm (E and F, green arrow) and pancreas (G and H, black arrow) is less affected. At 28–30 hpf, liver budding (shown as anterior endoderm thickening) was absent in *hdac3* MO (I vs. J, white arrow) as judged by *foxa3* expression and a reduced liver region was observed at 48 hpf (K, L). *foxa3* expression in pancreas region (I, J, black arrow and Pn in K, L) was less affected in both stages. Swim bladder was absent at 48 hpf in *hdac3* MO (K vs. L). Lv: liver; Pn: pancreas; in: intestine; Sb: swim bladder. Scale bar represents 100 μm in panels A–F; 50 μm in panels G–L.

stage in *hdac3* morphants, but *foxa3* expression in exocrine pancreas was less affected (Fig. 8K vs. L). *prox1* expression remained reduced in liver up to 5 dpf, indicating a small liver (data not shown). These phenotypes are similar to that of low concentration VPA-treated embryos. They confirmed *hdac3*'s role in early liver formation including hepatoblast specification and liver budding.

Since *hdac3* affects liver formation, we analyzed its expression pattern. As shown in Fig. S3, *hdac3* is widely expressed during the first day of embryonic development with high level expression in the brain. This expression pattern is similar to that of *hdac1* in the same period (Cunliffe, 2004). This wide-spread expression gradually becomes restricted in the anterior brain with very high expression in the eye. A low level expression was observed in the anterior endoderm at 2 dpf. By 3 dpf, high level expression in the intestinal bulb and low level expression in liver were observed while the expression in brain remains. By 5 dpf, it is expressed at high level in the intestine, but the liver expression disappears. VPA did not affect *hdac3* expression in the brain; however, it abolished *hdac3* expression in liver at 3 dpf and reduced its expression in the intestine from 3 dpf to 5 dpf (Figs. S3F, H and J).

The above results indicate that *hdac3* plays an important role in liver development. It is expressed transiently in the liver region and knockdown of its expression resulted in delay in liver development. Comparing to *hdac1*, zebrafish embryos can tolerate high amount of *hdac3* MO (3–4 times more than *hdac1* MO) without causing severe gross developmental defects or embryonic death while inhibiting liver formation and angiogenesis more profoundly and specifically.

Double knockdown of hdac1 and hdac3 leads to severe interruption of early embryonic development in zebrafish

To investigate the combined impact of double *hdac1* and *hdac3* knockdown, we injected both morpholinos together (3 ng/ml *hdac1* MO and 12 ng/embryo *hdac3* MO).

As shown in Fig. 9, double knockdown resulted in severe abnormalities in almost all embryos including no circulation, curved body, small head and severe cardiac hypertrophy, similar to *hadc1* single knockdown morphants (Fig. 9G). Severe angiogenesis defects in trunk blood vessels are observed in 90% of injected embryos ($n=200$), much more severe than single knockdown of either gene (Fig. 9D). No RFP+ liver could be detected at 3 dpf (Fig. 9G). These morphants could not survive more than 3 dpf. In contrast, control embryos (injected with same amount of 5 bp mismatch MOs) developed normally (Figs. 9A and B). It is noted that the amount of *hdac1*

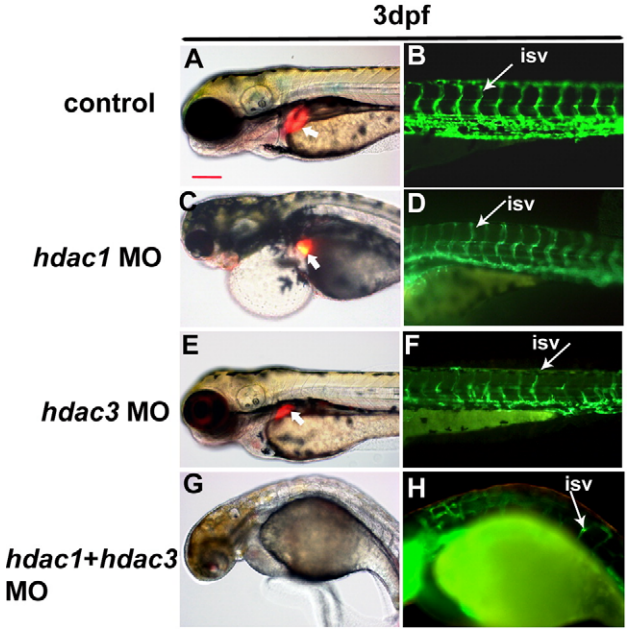

Fig. 9. Double knockdown of *hdac1* and *hdac3* leads to severe defects in embryonic development including liver and blood vessel. Double knockdown of *hdac1* and *hdac3* was performed by simultaneous injection of both MOs (*hdac1* MO at 3 ng/embryo; *hdac3* MO at 12 ng/embryo) into *Tg(lfabp:RFP; elaA:EGFP)* and *Tg(fli-1:EGFP)* embryos and was compared with the same quantity of 5 bp mismatch morpolinos (control, A–B). Liver (thick white arrow) was absent at 3 dpf and blood vessels (thin white arrow) were severely disrupted. Embryos were severely deformed in the double knockdown morphants (G, H) and they cannot survive beyond 3 dpf. All images were side view, with anterior to the left. Scale bar is 100 μm.

morpholino had to be reduced in the double knockdown experiments (3 ng/embryo) due to severe growth arrest and embryo death in early stages while *hdac1* single knockdown could tolerate MO dose of 6 ng/embryo. However, *hdac1* single knockdown using 3 ng/embryo MO generated morphological defects of similar severity as 6 ng/embryo MO (Figs. 6a and 9). These results indicate that both these *hdac* genes play critical roles in early zebrafish embryonic development including liver and vascular development.

Overexpression of hdac3 but not hdac1 partially rescued VPA induced liver defects in zebrafish embryos

To further confirm if VPA induced liver/exocrine pancreas defects mainly through suppressing *hdac3*, *hdac3* was over-expressed by mRNA microinjection (0.3 ng/embryo) into VPA-treated embryos. Under low concentration of VPA (10 μM), 60% (n=200) of the injected embryos were rescued to some extent in liver development (Fig. 10, compare B and F; Table 2). In contrast, injection of same amount of *hdac1* mRNA could only rescue about 4% (n=250) of embryos (Fig. 10, compare B and D; Table 2). Simultaneous injection of both *hdac1* and *hdac3* mRNA (0.3 ng/embryo of each mRNA) rescued the VPA liver phenotype to similar extent of *hdac3* mRNA alone (n=200) (Fig. 10, compare B and H; Table 2). Higher amount of

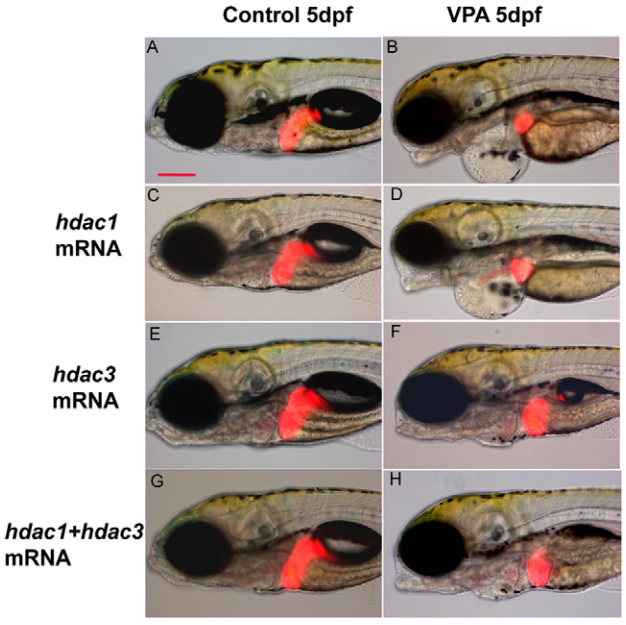

Fig. 10. *hdac3* mRNA partially rescued the liver defects in VPA-treated embryos while *hdac1* mRNA could not. 5′-capped mRNAs of *hdac1* and *hdac3* were synthesized in vitro and used to rescue the liver defects in VPA-treated embryos in Tg (*lfabp*:RFP, *elaA*:EGFP) by microinjection. Overexpression of *hdac1* mRNA (0.3 ng/embryo) did not generate any obvious impact on liver development (C vs. A) and *hdac1* mRNA failed to rescue the liver defects in VPA-treated embryos (D vs. B). In contrast, *hdac3* mRNA (0.3 ng/embryo) led to a slight increase in liver size compared to control (E vs. A). It also readily rescued the small liver defects in VPA-treated embryos although not to the same size of the control at the doses analyzed (F vs. B). Injection of both *hdac1* and *hdac3* mRNA together (0.3 ng/embryo each) rescued the liver defect under VPA to similar extent as *hdac3* mRNA alone (H vs. B). All images are lateral view of 5 dpf embryos, anterior toward the left. Scale bar is 100 μm.

Table 2
Summary of rescue effect of the small liver phenotype under VPA treatment by microinjection of *hdac1* or *hdac3* mRNA or both

	Without VPA		With VPA	
	No. of embryos	Liver size at 5dpf	No. of embryos	Liver size at 5 dpf
Control	300	Normal	350	Small (100%)
hdac1 mRNA (0.3 ng)	250	Normal	250	Not rescued, 242 (95%) Partial rescued, 8 (4%)
hdac3 mRNA (0.3 ng)	250	Marginally larger	200	Not rescued, 80 (40%) Partial rescued, 120 (60%)
hdac1+*hdac3* mRNA (0.3+0.3) ng	200	Normal	200	Not rescued, 80 (40%) Partial rescued, 120 (60%)

VPA used is 10 μM.

hdac1 or *hdac3* mRNA either singularly or together leads to severe abnormalities and embryonic death from early stages, making assessment of its effect on liver formation impossible. *hdac3* overexpression in control embryos generated a marginal but consistent increase in liver size while *hdac1* mRNA is less effective (Fig. 10, compare A vs. C, and A vs. E). Double injection of both mRNAs together into control embryos leads to marginal increase in liver size to similar extent as *hdac3* mRNA alone (Fig. 10G). These results confirmed that *hdac3* is more specifically required for liver development in zebrafish embryos. It is noted that, at higher VPA concentration (20 μM), *hdac3* overexpression could no longer rescue VPA induced liver defects (data not shown).

hdac3 promotes liver growth/expansion by suppressing growth differentiation factor 11 (gdf11) gene

It has been previously reported that HDAC3, but not other class I HDACs, specifically represses *gdf11* expression in cultured fibroblasts by deacetylating histone H3 on *gdf11* promoter (Zhang et al., 2004). HDAC inhibitor TSA has been shown to suppress HDAC3 expression which leads to up-regulation of *gdf11* gene in cell culture. The secreted Gdf11 is a member of the transforming growth factor β family that inhibits cell proliferation. It is involved in multiple developmental processes in mouse and chicken, including neurogenesis, chondrogenesis, myogenesis and pancreas development (Gamer et al., 2001; Harmon et al., 2004; Wu et al., 2003). However, its role in liver formation has not been studied in any species.

Using qRT-PCR, we observed that VPA up-regulated *gdf11* mRNA by at least 2-folds at 24 hpf, and up to 4-folds by 2 dpf. The up-regulation lowered to 2-folds at 3 dpf before returning back to control levels by 4 dpf (Fig. 11A).

Since *GDF11* is a direct and unique target of HDAC3 in cultured mammalian cells, it is possible that *hdac3* influences liver organogenesis in zebrafish embryos by targeting this gene. If so, knockdown of *gdf11* in *hdac3* morphants would be

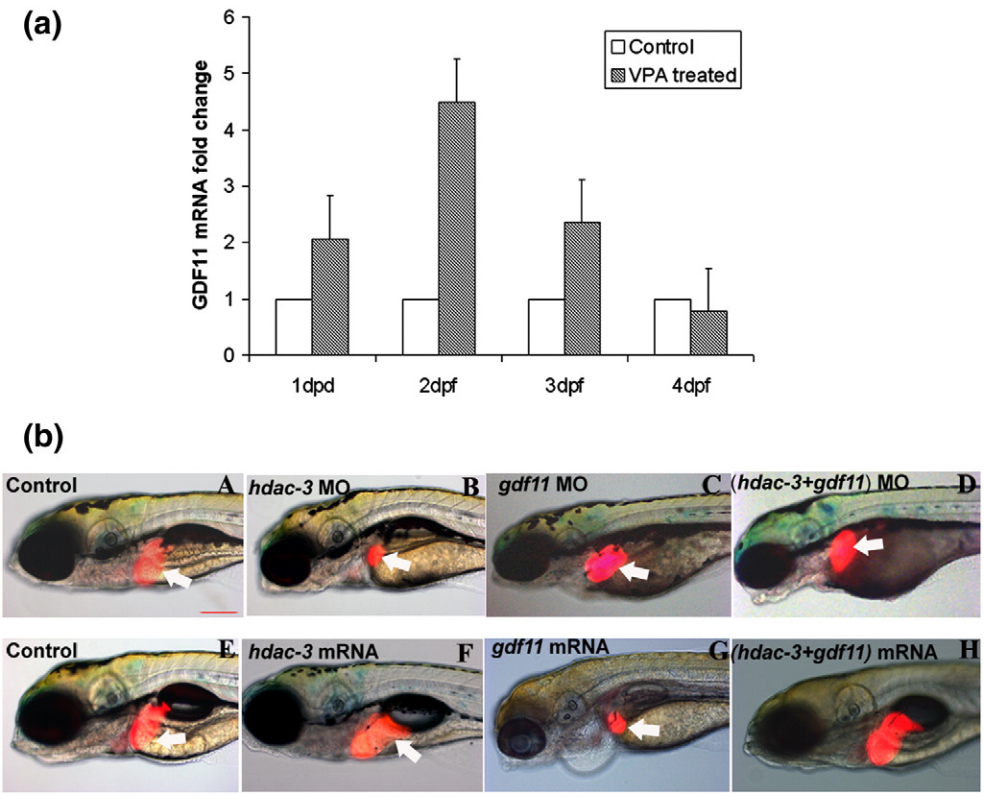

Fig. 11. (a) VPA induced *gdf11* expression in zebrafish embryos. WT zebrafish embryos were treated with VPA at shield stage and total RNA was extracted at various developmental stages. *gdf11* mRNA level was analyzed by real-time RT-PCR. *gdf11* mRNA level of the control embryos at each stage is set to be 1. (b) *gdf11* neutralized the liver defects induced by *hdac3*. To confirm that *hdac3* suppresses liver growth by suppressing *gdf11* gene, a double knockdown of *hdac3* and *gdf11* as well as simultaneous overexpression of both genes was performed. Knockdown of *gdf11* neutralized the effect of *hdac3* knockdown (D vs. B). On the other hand, overexpressions of *gdf11* lead to a small liver phenotype similar to *hdac3* morphants (G vs. E). Simultaneous overexpression of both genes leads to the neutralization of the liver phenotype induced by overexpression of *gdf11* alone (H vs. F), although liver in the double overexpression embryos was often not restored to the same size of the control (compare E and H). Liver is indicated by white arrow. All images are lateral view of 5 dpf embryos, anterior to the left. Scale bar is 100 μm.

expected to rescue/reverse the small liver phenotype. Indeed as shown in Fig. 11b, liver size was wholly or partially restored in about 40% ($n=50$) of embryos when *hdac3* and *gdf11* were knocked down simultaneously (compare panels B vs. D). Knockdown of *gdf11* alone showed no obvious impact on liver (Fig. 11b, panel C). On the other hand, overexpression of *gdf11* by mRNA microinjection generated a small liver phenotype at 5 dpf in a dose-dependent manner (Fig. 11b, panel G). About 10% of embryos were also much smaller in overall body size compared to control embryos when *gdf11* is overexpressed (data not shown). Interestingly, liver formed and developed normally in most of the *gdf11* overexpressed embryos up to 3 dpf (data not shown). Therefore, *gdf11* seems to be specifically involved in suppressing the growth/expansion phase of liver development in zebrafish, consistent with its role as a cell proliferation inhibitor. In contrast, *hdac3* overexpression leads to a slight increase in liver size (Fig. 11b, panel F vs. E). As expected, the small liver defects in *gdf11* overexpressed embryos were neutralized by simultaneous *hdac3* overexpression (Fig. 11b, panel H vs. G), consistent with the reported role of *hdac3* as a repressor of *gdf11* gene expression.

To confirm the role of *gdf11* in liver development, we analyzed its expression pattern. Overall, *gdf11* gene is expressed at very low levels and its expression further declined from 3 dpf onward, requiring prolonged staining to show positive signal. In VPA-treated embryos and *hdac3* morphants, *gdf11* expression in all domains was up-regulated (Figs. S4A and B). At 26–28 hpf, *gdf11* mRNA was localized to brain and eyes with no expression in the posterior part of the embryo (Fig. S4A). From 2 dpf onward, it is expressed in the pharyngeal arch region, the pectoral fin bud and several defined bilateral ventral areas anterior to the fin bud. By 4 dpf, expression in the notochord is obvious. Although no liver or pancreas expression could be detected in WT embryos in whole mount by WISH, expression was observed in liver at 48 hpf or in the adjacent mesoderm at 3 dpf under VPA by tissue sections (Figs. S4A, D' vs. D, F' vs. F). At 5 dpf, *gdf11* expression was essentially undetectable. No *gdf11* expression can be detected in embryos injected with *hdac3* mRNA in all stages, consistent with *hadc3* being a repressor of *gdf11* transcription (data not shown). All together, this expression pattern supports a link between *gdf11* and *hdac3* in zebrafish development.

gdf11 is involved in zebrafish exocrine pancreas development

GDF11 has been reported to regulate the production and maturation of islet progenitor cells in mouse endocrine pancreas development. One report showed that Gdf11 knockout mice

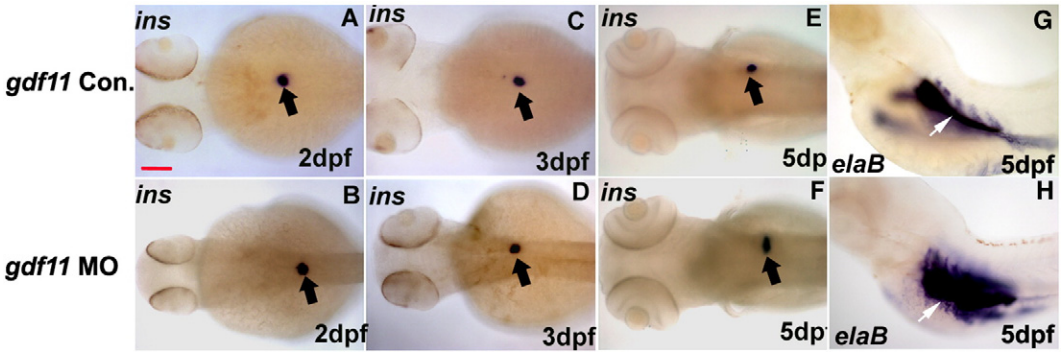

Fig. 12. *gdf11* negatively control exocrine pancreas growth in zebrafish. Pancreas formation was analyzed in *gdf11* morphants by *insulin* (A–F) and *elaB* (G–H) expression. The endocrine pancreas formation (black arrow) was basically normal in *gdf11* MO compared to 5 bp mismatch control morpholino injected embryos. A slight increase in insulin positive area was observed in about 10% of *gdf11* MO at 5 dpf (F). *elaB* positive exocrine pancreas (white arrow) showed obvious increase in the majority of *gdf11* MO at 5 dpf (H). Panels A–F are dorsal view while panels G–H are lateral view, anterior to the left. Scale bar is 100 μm.

harbor increased numbers of islet progenitor cells despite having a reduced mature β-cell numbers (Harmon et al., 2004). On the other hand, another report indicated a conflicting result of normal number of endocrine cells in these mice despite an increase in progenitors (Dichmann et al., 2006). We analyzed whether *gdf11* is involved in zebrafish pancreas development in *gdf11* morphants. Normal *insulin* expression in *gdf11* morphants showed that endocrine pancreas formation was generally not affected. Although *insulin* expressing cells were localized somewhat more posterior at 2 dpf in the trunk compared to 5 bp mismatch MO injected embryos (Figs. 12A and B; 80% of injected embryos, $n=50$), its expression and localization were similar to control at 3 dpf (Figs. 12C and D). At 5 dpf, a slightly larger endocrine pancreas was observed in about 10% of *gdf11* morphants ($n=50$) whereas the remaining embryos presented normal size endocrine pancreas (Figs. 12E and F). While exocrine pancreas formed at the normal developmental stage, an expanded *elaB* positive area was observed at 5 dpf in almost 80% of injected embryos ($n=100$) (Figs. 12G–H), suggesting a repressive role for *gdf11* in exocrine pancreas growth.

Discussion

In this work, we showed for the first time that HDACs are required for liver and exocrine pancreas development in zebrafish. Inhibiting HDACs by VPA interfered with early liver development including specification of endoderm cells to hepatoblasts, budding of liver primordium from anterior endoderm and differentiation of hepatoblasts to hepatocytes. In VPA-treated embryos, absence/delay of expression was observed for three undifferentiating liver markers (*hhex*, *prox1* and *foxa3*) and two liver differentiation makers (*Cp* and *lfabp*), indicating disruption of liver specification and differentiation. Transient VPA treatment from 6 hpf to 18 hpf leads to delay in liver development in *Tg(lfabp:RFP; elaA:EGFP*) embryos, with RFP+ liver first appearing at 4 dpf (Table 1A). When VPA was transiently present from 6 hpf to 24 hpf, 50% of embryos have no *hhex* expression at 32 hpf (Table 1B). These results demonstrate that HDACs are required for hepatoblast determination from endoderm in stages much earlier than the formation of its primordium around 24 hpf. Our results are consistent with the recent finding that *bmp* and *fgf* signaling is required for liver specification from 18 hpf to 24 hpf (Shin et al., 2007).

Under continuous VPA treatment, expression of *hhex*, *prox1* and *foxa3* in liver was observed from 48 hpf onward but *Cp* expression in liver was not observed until 4 dpf, demonstrating the presence of hepatoblasts at 2 dpf, but lack of differentiation of these cells until 4 dpf. When present from 24 hpf to 36 hpf transiently (hepatoblast already specified), 70% of embryos at 48 hpf lack *Cp* expression while a small Cp+ liver was observed the remaining embryos. However, liver size is nearly normal judged by *prox1* and *hhex* expression in these embryos. These results clearly indicate that VPA also suppressed hepatoblasts differentiation to hepatocytes, resulted in absence or less number of differentiated hepatocytes. They also show that endoderm cells remain competent to become hepatoblasts after 24 hpf and hepatoblasts remain competent to differentiate into hepatocytes after 4 dpf.

When present from 48 hpf to 60 hpf or 3 dpf (Cp+ hepatocytes already present), VPA leads to a small liver at 3 dpf (Tables 1A and B). Even though VPA is removed subsequently, liver still remains small up to 5 dpf. These results suggest that VPA either suppressed additional hepatoblast differentiation to Cp+ hepatocyte from 48 hpf onward, proliferation of Cp+ hepatocyte or both. Furthermore, inhibiting HDACs during 2–3 dpf seems to have a long lasting effect on subsequent liver growth/expansion, possibly through modulation of chromatin structure. When VPA is present from 3 dpf onward, liver developed normally and grew to normal size, suggesting a lack of inhibition on hepatocyte proliferation when HDACs are inhibited after 3 dpf. Further studies of hepatocyte proliferation under VPA are required to clarify if VPA also inhibited hepatocyte proliferation when present continuously or transiently between 2 dpf and 3 dpf.

We used VPA concentration at 20 μM or less which showed minimum developmental delay and no gross developmental defects during early developmental stages. The morphological features of the embryos before 3 dpf were comparable with control embryos (Fig. S1). Circulation was normal in treated embryos up to 4 dpf, and slowed down or stopped at 5 dpf in the

majority of the embryos (data not shown). The size of the embryos was comparable with untreated control up to 5 dpf. Therefore, the liver and exocrine pancreas defects observed in VPA-treated embryos were not due to the non-specific teratogenic or toxic affect. Indeed, VPA concentration less than 30 μM has been previously reported to be non-teratogenic in zebrafish embryo (Gurvich et al., 2005; Herrmann, 1993). We further showed that the liver defects are due to inhibition of HDACs using a structurally different HDAC inhibitor TSA and a non-active VPA analog valpromide.

VPA also effectively disrupted embryonic angiogenesis (Figs. 1 and 3). Similar although milder angiogenesis defects were observed in *hdac1* mutant, *hdac1* morphants (Pillai et al., 2004; Isenberg et al., 2007), and *hdac3* morphants (this work). Double knockdown of *hadc1* and *hadc3* generated severe angiogenesis defects, similar to high concentration VPA treatment (Fig. 9 and data not shown). These results demonstrate the importance of these two *hdacs* in embryonic blood vessel formation. Indeed, knockdown of *hdac1* gene suppressed about 75% of total HDAC activity while knockdown of *hdac3* leads to a reduction of about 25% of total HDAC activity in zebrafish embryos (Fig. 5). One possible mechanism through which VPA inhibits angiogenesis in zebrafish embryos is suppression of *vegf* expression (our unpublished data).

We demonstrated here that the liver defects induced by VPA in zebrafish embryos are not a result of its inhibition of angiogenesis. At similar level of angiogenesis inhibition, specific chemical angiogenesis inhibitors did not interfere with liver formation (Fig. 3). Altogether, these results supported a role of HDACs but not vascularization in liver formation. This is consistent with a previous report of normal liver budding in zebrafish *cloche* mutant in which the vasculature is severely defective (Field et al., 2003).

Through antisense MO knockdown, we further demonstrated that both *hdac1* and *hdac3* are required for liver formation. However, while *hdac1* is more globally required for embryogenesis, *hadc3* is more specifically required for liver formation. Similar to *hdac1* mutant, severe developmental defects were observed in *hdac1* morphants, consistent with the significant contribution of this gene to total HDAC enzymatic activity in zebrafish embryos (Fig. 5). On the other hand, knockdown of *hdac3* specifically perturbed liver formation without affecting pancreas development. In *hdac3* morphants, expressions of earlier liver markers (*hhex*, *prox1* and *foxa3*) as well as differentiation markers (*Cp* and *lfabp*) in liver region were delayed or reduced in similar fashion as in low concentration VPA (10 μM or 5 μM) -treated embryos, indicating the requirement of this gene in liver specification, budding and differentiation. In *hdac3* morphants, a small liver is present at 3 dpf. At 5 dpf, the number of liver cells was reduced to about 50% of control embryos (Fig. S2). However, since higher doses of VPA induced more severe defects in liver formation, it is likely that additional *hdacs* are also involved. Indeed, *hdac1* morphants also showed defects in liver growth (Fig. 6). However, due to more global function of *hdac1*, these morphants presented severe gross developmental defects from 3 dpf onward. It is possible that the liver defect in *hadc1* morphants is a secondary effect of other developmental defects in these embryos. To identify more target genes important for liver and pancreas development, a microarray approach has been adopted to identify genes influenced by low level VPA during a relevant developmental period (data will be presented elsewhere).

We further showed that *gdf11* is a possible target of *hdac3* in liver development in zebrafish. Knockdown of *gdf11* rescued the small liver phenotype in *hadc3* morphants (Fig. 11) while overexpression of *gdf11* suppressed liver growth, generating a small liver phenotype resembling *hdac3* morphants, possibly by suppressing hepatocyte proliferation (Fig. 11). Most importantly, overexpression of *hdac3* could partially rescue the liver growth defect in *gdf11* overexpressing embryos as well as in VPA-treated embryos, consistent with the result that *gdf11* mRNA expression was up-regulated by VPA. However, simultaneous overexpression of both *hadc1* and *hdac3* did not lead to more efficient rescue of VPA suppressed small liver phenotype. Since VPA inhibits multiple HDACs, it is possible that additional *hdac* genes in zebrafish are also involved. These results demonstrate the functional antagonism between *hdac3* and *gdf11*, suggesting that *hdac3* may promote liver growth by suppressing *gdf11* gene function in zebrafish. However, since liver formed normally up to 3 dpf in *gdf11* overexpressing embryos, it is clear that *hdac3* also functions through other target genes.

The Wnt/β-catenin pathway has been shown to be important in vertebrate liver morphogenesis and overexpression of β-catenin in chicken leads to 3-fold increase in liver weight (Suksaweang et al., 2004). In mouse, suppression of β-catenin resulted in reduced liver cell proliferation (Monga et al., 2003). Recently, mesodermal Wnt signaling was also shown to regulate liver specification in zebrafish (Ober et al., 2006). As HDAC inhibitors such as VPA have been shown to alter Wnt-dependent gene expression and regulate β-catenin pathway (Pillai et al., 2004; Wiltse, 2005), the induced defects in zebrafish liver formation could potentially involve alterations in Wnt signaling pathways as well.

Histone acetylation has been reported to be a checkpoint for transduction of FGF signals to induce mesoderm in *Xenopus* through transcription factor AP-1 (Xu et al., 2000). AP-1-mediated mesoderm induction in the animal caps is dramatically suppressed by the HDAC inhibitor TSA at a dose-dependent manner. Interestingly, this suppression can be rescued by ectopic expression of HDAC3 at early stage. Since Bmp and Fgf signaling is essential for liver specification in zebrafish (Shin et al., 2007), it will be interesting to know if *hdac3* function in early liver development is linked to Fgf.

VPA also interfered with exocrine pancreas formation. *elaB* expression normally starts from about 56 hpf and reach very high level in pancreas at 4 dpf (Mudumana et al., 2004). However, in VPA-treated embryos, *elaB* expression only appeared at 5 dpf. In contrast, the expression of endocrine pancreas marker *insulin* was normal, consistent with the model that the two parts of the pancreas derive from different progenitors and evolve differently during development. It has

been suggested that the mammalian liver and ventral pancreas arise from a common progenitor within the ventral foregut endoderm (Deutsch et al., 2001). Recently, fate map analysis of zebrafish pancreas confirmed that the dorsal pancreas (strictly endocrine) and ventral pancreas (primarily exocrine) come mostly from independent cell populations (Ward et al., 2007).

We did not detect any obvious changes in both endocrine and exocrine pancreas development in *hdac3* morphants (Fig. 7). Early endocrine pancreas development in *gdf11* morphants is also generally normal as indicated by insulin expression pattern (Fig. 12), although about 10% of morphants showed a slightly larger endocrine pancreas at this stage. However, exocrine pancreas was clearly enlarged at 5 dpf in *gdf11* morphants as judged by *elaB* expression pattern. As the pancreas phenotype in *gdf11* morphants only becomes obvious at 5 dpf, and the fact that the effectiveness of MO inhibition of gene expression declines quickly after 3 dpf, whether *hdac3* has any role in pancreas development needs to be further explored.

Recently, epigenetic modifications of DNA and histone by methylation have been shown to help execute specific developmental programs, affecting the terminal differentiation of intestine, exocrine pancreas and retina, but not endocrine pancreas and liver in zebrafish (Rai et al., 2006). Our data here clearly support the model that epigenetic modifications of histone/transcription factors by acetylation/deacetylation are also regulators of liver organogenesis.

Conclusion

We demonstrated for the first time that HDACs are required for early liver development in zebrafish embryos including specification, budding, and differentiation. They are also involved in exocrine pancreas formation but have no effect on the development of endocrine pancreas. While *hdac1* is more globally required for embryonic development including liver and exocrine pancreas, *hdac3* is more specifically required for liver formation. We further show that *hdac3* and *gdf11* function antagonistically in liver growth, consistent with earlier reports that *hdac3* negatively regulates *gdf11* transcription. *gdf11* also negatively regulates exocrine pancreas growth while its influence on endocrine pancreas is quite limited. In addition, we show that vascularization is not required for liver formation in zebrafish.

Acknowledgments

This work was supported by Singapore Biomedical Research Council grant BMRC/01/1/21/17/068. We thank the following people from the Department of Biological Sciences, National University of Singapore for their help: Dr. WK Chan for *prox1* probe, Dr. S Korzh for *Cp* probe and Ms. YL Wu for help in zebrafish maintenance.

Appendix A. Supplementary data

Supplementary data associated with this article can be found, in the online version, at doi:10.1016/j.ydbio.2008.02.034.

References

Cheung, W.L., Briggs, S.D., Allis, C.D., 2000. Acetylation and chromosomal functions. Curr. Opin. Cell Biol. 12, 326–333.

Cunliffe, V.T., 2004. Histone deacetylase 1 is required to repress Notch target gene expression during zebrafish neurogenesis and to maintain the production of motoneurones in response to hedgehog signalling. Development 131, 2983–2995.

Cunliffe, V.T., Casaccia-Bonnefil, P., 2006. Histone deacetylase 1 is essential for oligodendrocyte specification in the zebrafish CNS. Mech. Dev. 123, 24–30.

de Ruijter, A.J., van Gennip, A.H., Caron, H.N., Kemp, S., van Kuilenburg, A.B., 2003. Histone deacetylases (HDACs): characterization of the classical HDAC family. Biochem. J. 370, 737–749.

Deutsch, G., Jung, J., Zheng, M., Lora, J., Zaret, K.S., 2001. A bipotential precursor population for pancreas and liver within the embryonic endoderm. Development 128, 871–881.

Dichmann, D.S., Yassin, H., Serup, P., 2006. Analysis of pancreatic endocrine development in GDF11-deficient mice. Dev. Dyn. 235, 3016–3025.

Field, H.A., Ober, E.A., Roeser, T., Stainier, D.Y., 2003. Formation of the digestive system in zebrafish: I. Liver morphogenesis. Dev. Biol. 253, 279–290.

Gamer, L.W., Cox, K.A., Small, C., Rosen, V., 2001. Gdf11 is a negative regulator of chondrogenesis and myogenesis in the developing chick limb. Dev. Biol. 229, 407–420.

Gurvich, N., Berman, M.G., Wittner, B.S., Gentleman, R.C., Klein, P.S., Green, J.B., 2005. Association of valproate-induced teratogenesis with histone deacetylase inhibition in vivo. FASEB J. 19, 1166–1168.

Harmon, E.B., Apelqvist, A.A., Smart, N.G., Gu, X., Osborne, D.H., Kim, S.K., 2004. GDF11 modulates NGN3+ islet progenitor cell number and promotes beta-cell differentiation in pancreas development. Development 131, 6163–6174.

Her, G.M., Chiang, C.C., Chen, W.Y., Wu, J.L., 2003. In vivo studies of liver-type fatty acid binding protein (L-FABP) gene expression in liver of transgenic zebrafish (*Danio rerio*). FEBS Lett. 538, 125–133.

Herold, C., Ganslmayer, M., Ocker, M., Hermann, M., Geerts, A., Hahn, E.G., Schuppan, D., 2002. The histone-deacetylase inhibitor Trichostatin A blocks proliferation and triggers apoptotic programs in hepatoma cells. J. Hepatol. 36, 233–240.

Herrmann, K., 1993. Effects of the anticonvulsant drug valproic acid and related substances on the early development of the zebrafish (*Branchydanio rerio*). Toxicol. In Vitro 1, 41–54.

Isenberg, J.S., Jia, Y., Field, L., Ridnour, L.A., Sparatore, A., Del, S.P., Sowers, A.L., Yeh, G.C., Moody, T.W., Wink, D.A., Ramchandran, R., Roberts, D.D., 2007. Modulation of angiogenesis by dithiolethione-modified NSAIDs and valproic acid. Br. J. Pharmacol. 151, 63–72.

Isogai, S., Horiguchi, M., Weinstein, B.M., 2001. The vascular anatomy of the developing zebrafish: an atlas of embryonic and early larval development. Dev. Biol. 230, 278–301.

Korzh, S., Emelyanov, A., Korzh, V., 2001. Developmental analysis of ceruloplasmin gene and liver formation in zebrafish. Mech. Dev. 103, 137–139.

Lawson, N.D., Weinstein, B.M., 2002. In vivo imaging of embryonic vascular development using transgenic zebrafish. Dev. Biol. 248, 307–318.

Liang, D., Chang, J.R., Chin, A.J., Smith, A., Kelly, C., Weinberg, E.S., Ge, R., 2001. The role of vascular endothelial growth factor (VEGF) in vasculogenesis, angiogenesis, and hematopoiesis in zebrafish development. Mech. Dev. 108, 29–43.

Liao, W., Bisgrove, B.W., Sawyer, H., Hug, B., Bell, B., Peters, K., Grunwald, D.J., Stainier, D.Y., 1997. The zebrafish gene cloche acts upstream of a flk-1 homologue to regulate endothelial cell differentiation. Development 124, 381–389.

Liu, Y.W., Gao, W., Teh, H.L., Tan, J.H., Chan, W.K., 2003. Prox1 is a novel coregulator of Ff1b and is involved in the embryonic development of the zebra fish interrenal primordium. Mol. Cell. Biol. 23, 7243–7255.

Livak, K.J., Schmittgen, T.D., 2001. Analysis of relative gene expression data using real-time quantitative PCR and the 2(−Delta Delta C(T)) method. Methods 25, 402–408.

Marks, P.A., Miller, T., Richon, V.M., 2003. Histone deacetylases. Curr. Opin. Pharmacol. 3, 344–351.

Mendel, D.B., Schreck, R.E., West, D.C., Li, G., Strawn, L.M., Tanciongco, S.S., Vasile, S., Shawver, L.K., Cherrington, J.M., 2000. The angiogenesis inhibitor SU5416 has long-lasting effects on vascular endothelial growth factor receptor phosphorylation and function. Clin. Cancer Res. 6, 4848–4858.

Michaelis, M., Michaelis, U.R., Fleming, I., Suhan, T., Cinatl, J., Blaheta, R.A., Hoffmann, K., Kotchetkov, R., Busse, R., Nau, H., Cinatl Jr., J., 2004. Valproic acid inhibits angiogenesis in vitro and in vivo. Mol. Pharmacol. 65, 520–527.

Monga, S.P., Monga, H.K., Tan, X., Mule, K., Pediaditakis, P., Michalopoulos, G.K., 2003. Beta-catenin antisense studies in embryonic liver cultures: role in proliferation, apoptosis, and lineage specification. Gastroenterology 124, 202–216.

Mudumana, S.P., Wan, H., Singh, M., Korzh, V., Gong, Z., 2004. Expression analyses of zebrafish transferrin, ifabp, and elastaseB mRNAs as differentiation markers for the three major endodermal organs: liver, intestine, and exocrine pancreas. Dev. Dyn. 230, 165–173.

Nasevicius, A., Larson, J., Ekker, S.C., 2000. Distinct requirements for zebrafish angiogenesis revealed by a VEGF-A morphant. Yeast 17, 294–301.

Ober, E.A., Verkade, H., Field, H.A., Stainier, D.Y., 2006. Mesodermal Wnt2b signalling positively regulates liver specification. Nature 442, 688–691.

Phiel, C.J., Zhang, F., Huang, E.Y., Guenther, M.G., Lazar, M.A., Klein, P.S., 2001. Histone deacetylase is a direct target of valproic acid, a potent anticonvulsant, mood stabilizer, and teratogen. J. Biol. Chem. 276, 36734–36741.

Pillai, R., Coverdale, L.E., Dubey, G., Martin, C.C., 2004. Histone deacetylase 1 (HDAC-1) required for the normal formation of craniofacial cartilage and pectoral fins of the zebrafish. Dev. Dyn. 231, 647–654.

Rai, K., Nadauld, L.D., Chidester, S., Manos, E.J., James, S.R., Karpf, A.R., Cairns, B.R., Jones, D.A., 2006. Zebra fish Dnmt1 and Suv39h1 regulate organ-specific terminal differentiation during development. Mol. Cell. Biol. 26, 7077–7085.

Shin, D., Shin, C.H., Tucker, J., Ober, E.A., Rentzsch, F., Poss, K.D., Hammerschmidt, M., Mullins, M.C., Stainier, D.Y., 2007. Bmp and Fgf signaling are essential for liver specification in zebrafish. Development 134, 2041–2050.

Stainier, D.Y., Weinstein, B.M., Detrich III, H.W., Zon, L.I., Fishman, M.C., 1995. Cloche, an early acting zebrafish gene, is required by both the endothelial and hematopoietic lineages. Development 121, 3141–3150.

Suksaweang, S., Lin, C.M., Jiang, T.X., Hughes, M.W., Widelitz, R.B., Chuong, C.M., 2004. Morphogenesis of chicken liver: identification of localized growth zones and the role of beta-catenin/Wnt in size regulation. Dev. Biol. 266, 109–122.

Tou, L., Liu, Q., Shivdasani, R.A., 2004. Regulation of mammalian epithelial differentiation and intestine development by class I histone deacetylases. Mol. Cell. Biol. 24, 3132–3139.

Wallace, K.N., Yusuff, S., Sonntag, J.M., Chin, A.J., Pack, M., 2001. Zebrafish hhex regulates liver development and digestive organ chirality. Genesis 30, 141–143.

Wan, H., Korzh, S., Li, Z., Mudumana, S.P., Korzh, V., Jiang, Y.J., Lin, S., Gong, Z., 2006. Analyses of pancreas development by generation of gfp transgenic zebrafish using an exocrine pancreas-specific elastaseA gene promoter. Exp. Cell Res. 312, 1526–1539.

Ward, A.B., Warga, R.M., Prince, V.E., 2007. Origin of the zebrafish endocrine and exocrine pancreas. Dev. Dyn. 236, 1558–1569.

Westerfield, M., 1995. The Zebrafish Book. University of Oregon Press, Eugene, USA.

Whetstine, J.R., Ceron, J., Ladd, B., Dufourcq, P., Reinke, V., Shi, Y., 2005. Regulation of tissue-specific and extracellular matrix-related genes by a class I histone deacetylase. Mol. Cell 18, 483–490.

Wilson, A.J., Byun, D.S., Popova, N., Murray, L.B., L'Italien, K., Sowa, Y., Arango, D., Velcich, A., Augenlicht, L.H., Mariadason, J.M., 2006. Histone deacetylase 3 (HDAC3) and other class I HDACs regulate colon cell maturation and p21 expression and are deregulated in human colon cancer. J. Biol. Chem. 281, 13548–13558.

Wiltse, J., 2005. Mode of action: inhibition of histone deacetylase, altering WNT-dependent gene expression, and regulation of beta-catenin—developmental effects of valproic acid. Crit. Rev. Toxicol. 35, 727–738.

Wu, H.H., Ivkovic, S., Murray, R.C., Jaramillo, S., Lyons, K.M., Johnson, J.E., Calof, A.L., 2003. Autoregulation of neurogenesis by GDF11. Neuron 37, 197–207.

Xu, R.H., Peng, Y., Fan, J., Yan, D., Yamagoe, S., Princler, G., Sredni, D., Ozato, K., Kung, H.F., 2000. Histone acetylation is a checkpoint in FGF-stimulated mesoderm induction. Dev. Dyn. 218, 628–635.

Yamaguchi, M., Tonou-Fujimori, N., Komori, A., Maeda, R., Nojima, Y., Li, H., Okamoto, H., Masai, I., 2005. Histone deacetylase 1 regulates retinal neurogenesis in zebrafish by suppressing Wnt and Notch signaling pathways. Development 132, 3027–3043.

Yamashita, Y., Shimada, M., Harimoto, N., Rikimaru, T., Shirabe, K., Tanaka, S., Sugimachi, K., 2003. Histone deacetylase inhibitor trichostatin A induces cell-cycle arrest/apoptosis and hepatocyte differentiation in human hepatoma cells. Int. J. Cancer 103, 572–576.

Zaret, K.S., 2002. Regulatory phases of early liver development: paradigms of organogenesis. Nat. Rev., Genet. 3, 499–512.

Zgouras, D., Becker, U., Loitsch, S., Stein, J., 2004. Modulation of angiogenesis-related protein synthesis by valproic acid. Biochem. Biophys. Res. Commun. 316, 693–697.

Zhang, X., Wharton, W., Yuan, Z., Tsai, S.C., Olashaw, N., Seto, E., 2004. Activation of the growth-differentiation factor 11 gene by the histone deacetylase (HDAC) inhibitor trichostatin A and repression by HDAC3. Mol. Cell. Biol. 24, 5106–5118.